

# Assumption of Fixed Ball at the Centre of Mass of the Hand Results in Underestimation of Wrist Muscle Flexion Torque Component Owing to Ball Kinetics Immediately before Ball Release in Baseball Throwing

Takeji Kojima

Chofu Biomechanics Laboratory, Tokyo, Japan  
Email: [cookingkumasan@tbz.t-com.ne.jp](mailto:cookingkumasan@tbz.t-com.ne.jp)

**How to cite this paper:** Kojima, T. (2025). Assumption of Fixed Ball at the Centre of Mass of the Hand Results in Underestimation of Wrist Muscle Flexion Torque Component Owing to Ball Kinetics Immediately before Ball Release in Baseball Throwing. *Advances in Physical Education*, 15, 254-285. <https://doi.org/10.4236/ape.2025.152020>

**Received:** April 5, 2025

**Accepted:** May 28, 2025

**Published:** May 31, 2025

Copyright © 2025 by author(s) and Scientific Research Publishing Inc. This work is licensed under the Creative Commons Attribution International License (CC BY 4.0).

<http://creativecommons.org/licenses/by/4.0/>



Open Access

---

## Abstract

In conventional inverse dynamics analyses of the human body, the locations of the centre of pressure (COP) of external forces acting on the body segments are necessary to solve problems. In the analysis of baseball throwing, the location of the COP of the forces acting from the baseball on the palm and/or fingers remains unclear, and the centre of mass (COM) of the ball may be fixed at a point in the hand until ball release: at the COM or third metacarpal joint of the hand, for instance. This study aimed to investigate possible errors of the muscle flexion torque at the wrist joint due to an assumption that a ball is fixed at the COM of the hand until ball release in baseball throwing. Seven male collegiate baseball players each threw a baseball with their supreme effort at a target in a laboratory. The markers attached to the throwing arm and ball were captured at 500 fps with eight cameras of a motion capture system. Wrist muscle flexion torques were determined using an inverse dynamics analysis, which does not necessitate the COP location, under the following two conditions: an actual ball position and motion were considered (C1), and the COM of the ball was fixed at the COM of the hand until the release (C2). The torque determined under C1 was significantly different from ( $p < 0.001$ ) and larger than that determined under C2 at the same sampling time for 0.038 s immediately before the release for each participant. Thus, kinematic information of the actual ball and analysis could be important and useful for elucidating the wrist joint mechanics in baseball throwing. This study comprehensively discusses the reasons for the differences between the results determined under C1 and C2.

---

---

## Keywords

Baseball Throwing, Wrist Joint, Non-Conventional Inverse Dynamics, Non-Fixed Ball at Hand

---

## 1. Introduction

In researches concerning baseball throwing, [Feltner & Dapena \(1986\)](#) may be the first researchers who have analysed the kinetics of the shoulder, elbow, and wrist joints of the throwing arm in three dimensions (3D), although the results of the wrist joint were not published. The authors have reported on the joint torques (moments of muscle and connective tissue forces) and joint forces at the shoulder and elbow joints as well as their kinematics in 3D. The authors represented the throwing arm as a four segment model composed of the upper arm, forearm, hand, and baseball, and these segments were rigid bodies. Since they assumed the force acting from the palm and/or fingers on the ball passed through its centre of mass (COM), the ball was treated as a mass point, or its angular acceleration was zero. In determining the muscle torque at the wrist joint, which was necessary for determining the muscle torques at the elbow and shoulder joints with their methods, they did not use the location of the centre of pressure (COP) of the forces acting from the ball on the palm and/or fingers. They assumed the force acting from the ball on the hand was the reaction to the force made by the hand on the ball. [Feltner \(1989\)](#) has reported on the mechanisms of how the upper arm and forearm motions were produced by body actions and the muscle torques at the shoulder and elbow joints in baseball throwing. In this research, a set of the forearm, hand, and baseball was considered a rigid body, and thus, the angle of the wrist joint was constant throughout a throw ([Feltner & Dapena, 1989](#)). The ball was also treated as a mass point. The relative positional relationship among the three segments of the set was the average of the relationships throughout each throw. [Sakurai et al. \(1990\)](#) may be the first researchers who have reported on the kinematics of the wrist joint as well as the shoulder and elbow joints of the throwing arm in baseball throwing in 3D. [Sakurai et al. \(1993\)](#) have reported on the kinematic differences between the motions of the wrist, elbow, and shoulder joints of the throwing arm in fastball and curveball in 3D. [Miyanishi et al. \(1997\)](#) may be the first researchers who have reported on the kinetics of the wrist joint as well as the shoulder and elbow joints of the throwing arm in baseball throwing in 3D. In addition, the authors have reported on the energy flows due to the joint torques and forces at the three joints from the upper torso to the baseball. The authors assumed that the baseball was a mass point, and that the COM of the ball was fixed at the COM of the hand until ball release.

In researches concerning the joint kinetics of the throwing arm in baseball throwing, some researchers have determined muscle torques around the wrist joint of the arm using conventional inverse dynamics analyses ([Robertson et al.,](#)

2014) assuming that the COM of a baseball is fixed at a point in the hand until ball release: at the COM of the hand (Miyanishi et al., 1997; Hirashima et al., 2007; Hirashima et al., 2008), at the centre of the third metacarpophalangeal (MP) joint (Fleisig et al., 2006; Dun et al., 2008; Naito & Maruyama, 2008; Naito et al., 2014), at the distal part of the second metacarpal (O'Connell et al., 2022), and at an unknown point of the hand (Tanaka et al., 2020; Gomaz et al., 2024). However, the COM of the ball does not occupy the points of the hand stated above, and the ball actually rolls along the fingers toward their chips immediately before the release. Hence, the joint torques determined on the assumption may have errors owing to the assumption.

In solving the inverse problem of the throwing arm in baseball throwing using the conventional inverse dynamics analysis, it is assumed that the hand, forearm, upper arm, and upper trunk are linked rigid bodies, and that the location of the COP of the forces acting from a body on the adjacent body is the centre of the joint made by the two bodies. However, the location of the COP of the forces acting from the ball on the hand is not determined simply because a baseball does not link with the hand. If the location is determined, the Newton-Euler equations (Zatsiorsky, 2002) are applied to a rigid body recursively from the ball to the upper arm. The assumption that the COM of a baseball is fixed at a point of the hand until ball release may have been used owing to the difficulty in determining the location precisely. Hof (1992) has reported a simple inverse dynamics analysis method which does not necessitate the location of the COP of the forces acting from the ball to the palm and/or fingers of the throwing arm in baseball throwing, thus allowing the adoption of an actual ball position and motion data during the throwing. One of the points of the method is that the equations are applied not to a rigid body but to a set of contiguous rigid bodies (Supplementary Material, S5).

This study aimed to investigate the muscle flexion torque at the wrist joint in baseball throwing under two conditions using the analysis method reported by Hof (1992), and to elucidate sources of the possible differences between the torques determined under the conditions. The first condition (C1) was that an actual ball position including ball rolling along the fingers was considered, and the second (C2) was that the COM of the ball was assumed to be fixed at the COM of the hand until ball release. The hypothesis of this study was that the value of the muscle flexion torque at the wrist joint determined under C1 was significantly different from that of the torque determined under C2 at the same sampling time for a short period immediately before ball release.

## 2. Methods

### Participants

Seven right-handed male collegiate baseball players (*a - g*) voluntarily participated in this study. The age (mean  $\pm$  standard deviation [SD]), height, and body mass of the participants were  $20.5 \pm 0.8$  years,  $1.73 \pm 0.03$  m, and  $71.2 \pm 9.1$  kg, respectively. They had  $9.9 \pm 3.2$  years of experience in playing baseball (Table 1).

In accordance with the Declaration of Helsinki, the purposes of this research and experimental procedure were explained to the participants in written and oral forms. Written informed consent was obtained from each participant prior to the experiment.

**Table 1.** Mean age, height, body mass, and experience in playing baseball.

Age	20.5 ± 0.8 years.
Height	1.73 ± 0.03 m.
Body mass	71.2 ± 9.1 kg.
Experience	9.9 ± 3.2 years.

#### Markers and measurement of the hand

Retroreflective spherical markers of three kinds of diameters (8, 10 and 15 mm) were attached to or near body landmarks of the throwing arm (**Figure 1**). The markers for the first finger were attached to it only for the first two participants, *a* and *b* (**Figure 1(a)**). The markers attached to or near the following body landmarks were used for the motion analysis as follows: the medial and lateral epicondyles (15 mm), radius and ulnar styloid processes (10 mm), dorsal head of the third metacarpal (10 mm), medial and lateral sides of the distal interphalangeal joints (8 mm) of the second and third fingers, and nails (8 mm) of the fingers. Three retroreflective and hemispherical markers (15 mm) were attached to the ball. The imaginary straight line connecting the first two markers passed through the centre of the ball, and the third marker was near the midpoint of a circular line connecting the first two markers along the surface of the ball. The thickness of the head of the third metacarpal was measured with a vernier caliper (Digital Caliper 19975, Shinwa Rules, Tsubame, Japan). The length from the distal end of the head to the centre of the wrist joint was measured using the caliper. The thickness of the part of the distal phalanx to which the markers were attached was measured for each of the second and third fingers. The length from the tip of the finger to the centre of the distal interphalangeal joint was measured for both fingers.

#### Task

Each participant wore a short sleeved T-shirt, shorts and rubber-soled sport shoes, and threw a baseball (0.072 m and 0.151 kg in diameter and mass, respectively) to a square target (0.2 m on a side) hung on a small backstop 25 times with his supreme effort on a flat floor in a laboratory. The participant was instructed to throw a four-seam fastball as fast as possible, and make the ball hit the target putting his rear foot on a line marked on the floor at the start of the throwing. The height of the target centre was adjusted to the eye level of each participant when standing on the floor. The distance from the line to the backstop was approximately 3.4 m. The markers were attached to the body segments of the participant after he felt that he had sufficiently practiced. The marker at the medial side of the proximal interphalangeal joint of the third finger (**Figure 1**) was removed from

the finger after the motion capture of the static posture of the throwing arm. Then, the participant threw the ball several times before the start of the motion capture of the throwing.

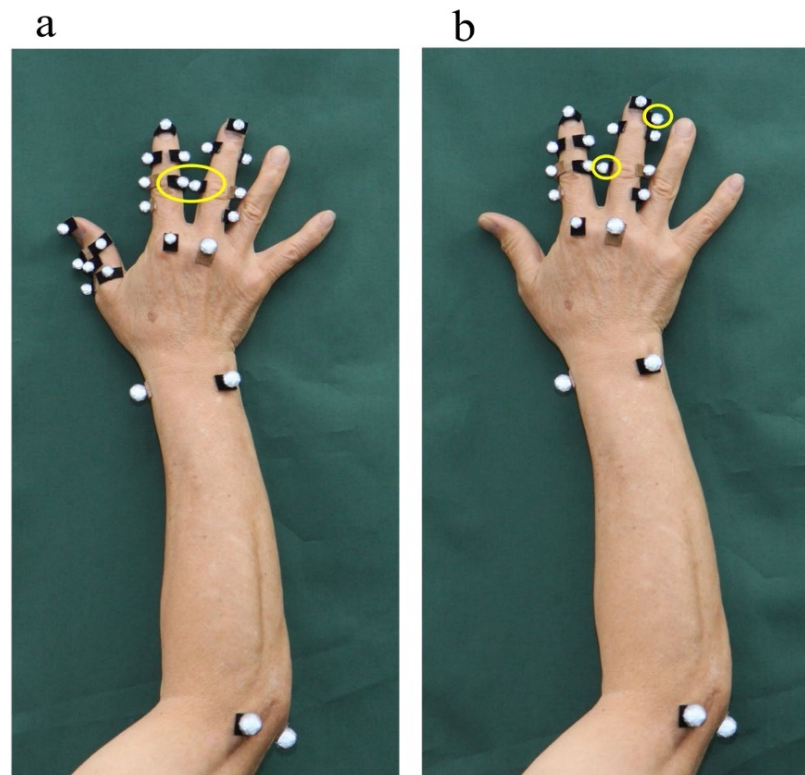


**Figure 1.** Marker sets for the participants *a* and *b* (a), and for the participant *c* to participant *g* (b).

#### Motion capture and coordinate systems

The static posture and throwing motion of the throwing arm were captured with eight cameras (MT-10, Vicon Motion Systems, Oxford, UK) at 500 fps. The coordinates of the markers were filtered using a fourth order no-delay Butterworth typed digital low-pass filter with a cut-off frequency of 100 Hz after post-cleaning of the coordinates (Nexus 1.8.5, Vicon Motion Systems, Oxford, UK). The global coordinate systems used in this paper were right-handed orthogonal coordinate systems composed of unit vectors. The origin of the coordinate system of the laboratory was at the centre of the line on which each participant put his rear foot. The y-axis of the system was parallel to the floor and directed to the target, and the z-axis was vertically directed upward. The x-axis was the cross product (Supplementary Material S1) of y- and z-axes. The local coordinate systems of the forearm and hand were defined using the markers attached to the body segments. The axes of the systems were parallel to their matching x-, y- and z-axes of **Table 2**. The local coordinate system of the wrist joint was the same with that of the forearm (**Figure 2**). The systems of the body segments in the static posture were determined using the definitions of both body segments.

**Table 2.** Definitions of the local coordinate systems of the forearm and hand. The local coordinate system of the wrist joint is the same with that of the forearm, and the y- and z-axes of the wrist joint are flexion-extension and radial-ulnar deviation axes, respectively.

Forearm	
x-axis	from the midpoint of the markers at the medial and lateral epicondyles to the midpoint of the markers at the radius and ulnar styloid processes.
y-axis	cross product of z- and x-axes
z-axis	cross product of x- and y'-axes.
y'-axis	from the marker at the ulnar styloid process to that of the radius styloid process.
Hand	
x-axis	from the midpoint of the markers at the radius and ulnar styloid processes to the centre of the third metacarpal joint.
y-axis	cross product of z- and x-axes.
z-axis	cross product of x- and y'-axes.
y'-axis	from the marker at the ulnar styloid process to that of the radius styloid process.

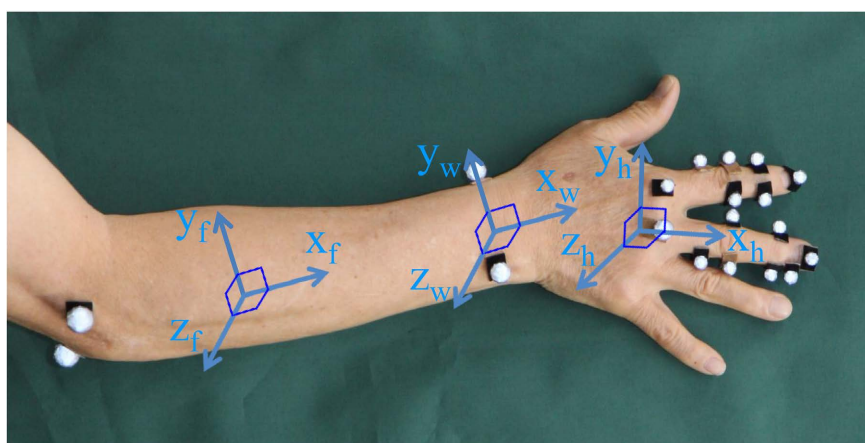


**Figure 2.** Local coordinate systems of the forearm, wrist joint, and hand of the right arm. The subscripts f, w, and h indicate the forearm, wrist joint, and hand, respectively.

### Kinematics

The centres of the elbow and wrist joints were estimated as the midpoints of the markers at the medial and lateral epicondyles, and those at the radial and ulnar styloid processes, respectively. The centre of the third MP joint was determined using the coordinates of the markers at the third dorsal head of metacarpal and the medial and lateral styloid processes considering the thickness of the head, radius of the marker on the head, and length of the line connecting the centres of the marker and the wrist joint after [Barrentine et al. \(1998\)](#). The tips of the second and third fingers were determined similarly for the third MP joint centre: the markers on the nail and on both sides of the distal interphalangeal joint, and the length from the tip to the centre of the joint were used for the determination for each finger. The COM of the hand was determined after [Ae et al. \(1992\)](#). The location of the COM was 89.1% of the distance from the centre of the wrist joint to that of the third MP joint. The COM of the hand used hereafter is this COM in

accordance with those in previous researches (Miyaniishi et al., 1997; Hirashima et al., 2007; Hirashima et al., 2008; Debicki et al., 2011). The centre of the ball was determined as the midpoint of the first two hemispherical markers attached to the ball.

The coordinates of the following markers were used to determine the rotation matrices of the local coordinate systems of the forearm and hand: the markers at the lateral epicondyle and radial and ulnar processes, and the latter two markers and marker on the head of the third metacarpal, respectively. The rotation matrix of the ball was determined using the coordinates of the three markers on the ball. The rotation matrices of the body segments and ball were determined using the Fortran program DISP3D, which was available on the ISB website (<https://isbweb.org/>), after the algorithm by Veldpaus et al. (1988): DISP3DB is the new version of the program now. The attitudes of the local coordinate systems of the forearm and hand during the throwing were determined through the multiplication of the rotation matrices from the left side with their matching attitude matrices determined in the static posture. The angular velocities of the body segments and ball were determined with their rotation matrices using Poisson's equation (Zatsiorsky, 1998). The velocities and accelerations of the COMs of the hand and ball, and the angular accelerations of the hand and ball were determined using numerical differentiations. The angular velocity and angular acceleration of the ball under C2 were assumed to be the same with the angular velocity and angular acceleration of the hand, respectively.

The frame of ball release was determined as the frame next to that in which the distance between the centre of the ball and tip of the second finger was the shortest around the release in each throw.

#### Kinetics

The muscle torque at the wrist joint was resolved into six elements depicted as the following equations after the equation (7) in Hof (1992) (Figure 3, Supplementary Material S1, S2, S4, S5):

$$\begin{aligned} \mathbf{T}_1 = & \mathbf{r}_b \times m_b \mathbf{a}_b + d(I_b \boldsymbol{\omega}_b)/dt - \mathbf{r}_b \times m_b \mathbf{g} \\ & + \mathbf{r}_h \times m_h \mathbf{a}_h + d(I_h \boldsymbol{\omega}_h)/dt - \mathbf{r}_h \times m_h \mathbf{g} \end{aligned} \quad (1)$$

$$\begin{aligned} \mathbf{T}_2 = & \mathbf{r}_h \times m_b \mathbf{a}_h + d(I_b \boldsymbol{\omega}_h)/dt - \mathbf{r}_h \times m_b \mathbf{g} \\ & + \mathbf{r}_h \times m_h \mathbf{a}_h + d(I_h \boldsymbol{\omega}_h)/dt - \mathbf{r}_h \times m_h \mathbf{g} \end{aligned} \quad (2)$$

where  $\mathbf{T}_1$  and  $\mathbf{T}_2$  are the vectors of the muscle torques at the wrist joint for C1 and C2, respectively,  $m_b$  and  $m_h$  are the mass of the ball and hand, respectively,  $t$  is time,  $I_b$  and  $I_h$  are the inertia tensors of the ball and hand, respectively,  $\mathbf{g}$  is the acceleration vector due to gravity,  $\mathbf{r}_b$  and  $\mathbf{r}_h$  are the position vectors from the wrist joint centre to the COMs of the ball and the hand, respectively,  $\mathbf{a}_b$  and  $\mathbf{a}_h$  are the acceleration vectors of the COMs, respectively,  $\boldsymbol{\omega}_b$  and  $\boldsymbol{\omega}_h$  are the angular velocity vectors of the ball and hand, respectively, and  $\times$  indicates the cross product of vectors (Supplementary Material S1).

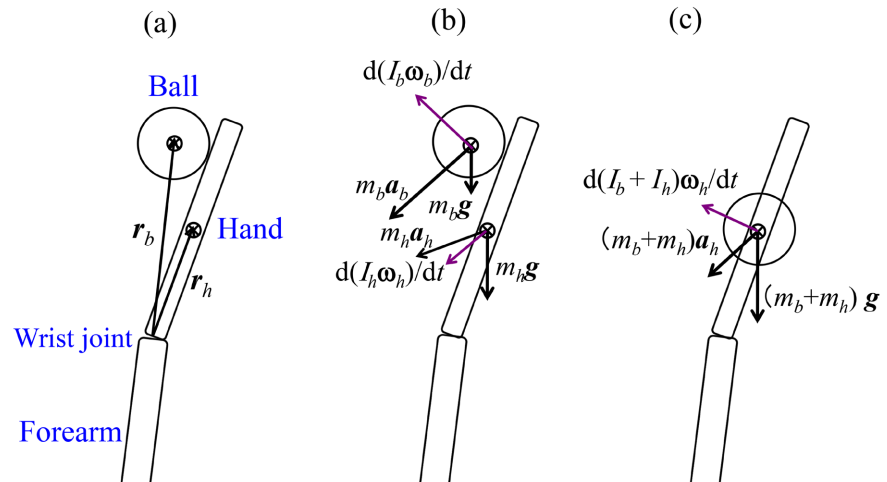


**Figure 3.** Explanations of the vectors concerning equations (1) and (2). (a) position vectors  $\mathbf{r}_b$ , and  $\mathbf{r}_h$ . (b) force and torque vectors used under C1. (c) force and torque vectors used under C2.

$d(I_b\boldsymbol{\omega}_b)/dt$  and  $d(I_h\boldsymbol{\omega}_h)/dt$  were determined in the global coordinate system and the local of the hand, respectively (Supplementary Material S4). The principal moment of inertia of the hand was determined using the values of radius of gyration reported by [Ae et al. \(1992\)](#). The values for x-, y-, and z-axes of the local coordinate system of the hand ([Figure 2](#)) were 0.314, 0.519, and 0.571, respectively. The torque needed to accelerate the hand angularly around its COM was determined using Euler dynamic equations ([Greenwood, 1988](#)) (Supplementary Materials S4). The ball was considered a homogeneous sphere in determining  $I_b$ . The first and last three terms on the right side of Equations (1) and (2) were the torque components from the ball kinetics and hand kinetics, respectively. The possible difference between the muscle torques at the wrist joint determined under C1 and C2 was attributable only to the difference between the ball kinetics determined under the two conditions because the same hand motion was analysed under both conditions, or the last three terms of Equation (1) are equal to their matching terms of Equation (2).

$\mathbf{T}_1$ ,  $\mathbf{T}_2$ , and the first three terms on the right side of Equation (1),  $\mathbf{r}_b \times m_b\mathbf{a}_b$ ,  $d(I_b\boldsymbol{\omega}_b)/dt - \mathbf{r}_b \times m_b\mathbf{g}$ , and the terms of Equation (2),  $\mathbf{r}_h \times m_b\mathbf{a}_b$ ,  $d(I_b\boldsymbol{\omega}_b)/dt - \mathbf{r}_h \times m_b\mathbf{g}$  were projected along the flexion-extension axis of the wrist joint (Supplementary Material S3). The projected components of these vectors of the first three terms and the sum of the components are called the element due to ball acceleration (E1), the element due to ball angular acceleration (E2), the element due to gravity on the ball (E3), and the sum of the elements (SUM), respectively. The position vector from the centre of the elbow joint to that of the wrist  $\mathbf{r}_{fa}$ ,  $\mathbf{r}_b$ ,  $\mathbf{r}_h$ ,  $m_b\mathbf{a}_b$ , and  $m_b\mathbf{a}_h$  were projected onto a plane perpendicular to the wrist flexion-extension axis in a throw and are presented as  $\mathbf{r}'_{fa}$ ,  $\mathbf{r}'_b$ ,  $\mathbf{r}'_h$ ,  $m_b\mathbf{a}'_b$  and  $m_b\mathbf{a}'_h$ , respectively. The value of the magnitude of the cross product  $\mathbf{r}'_b \times m_b\mathbf{a}'_b$  is equal to the value of  $|\mathbf{r}'_b| \cdot |m_b\mathbf{a}'_b| \cdot |\sin\theta_1|$ , where  $\theta_1$  is the angle between  $\mathbf{r}'_b$  and  $m_b\mathbf{a}'_b$ .

The value of  $|\mathbf{r}'_b| \cdot |m_b \mathbf{a}'_b| \cdot \sin \theta_1$  is equal to that of the element due to ball acceleration under C1 because these vectors were obtained through the projection onto the plane perpendicular to the wrist flexion-extension axis (Supplementary Material S3). The value of  $\sin \theta_1$  was determined as the ratio of the value of the magnitude of  $\mathbf{r}'_b \times m_b \mathbf{a}'_b$  along the axis to that of  $|\mathbf{r}'_b| \cdot |m_b \mathbf{a}'_b|$  considering the sign of  $\mathbf{r}'_b \times m_b \mathbf{a}'_b$ . The value of  $\sin \theta_2$  which was the sine of the angle between  $\mathbf{r}'_b$  and  $m_b \mathbf{a}'_b$  was determined in a similar way to the value of  $\sin \theta_1$ .  $\mathbf{T}_1$ ,  $\mathbf{T}_2$ , and both the first three terms on the right side of Equations (1) and (2) were also projected along the radial-ulnar deviation axis of the wrist joint. The projected three terms are called similarly to the projected three terms along the flexion-extension axis.

The frames from at least 0.060 s before ball release to at least 0.020 s after the release were used for motion analysis for each throwing trial. The trial in which the retroreflective marker(s) needed for kinetic analysis dropped from the participant's body segments or the coordinates of the marker(s) were not estimated using the algorithm of the Nexus 1.8.5 (Vicon Motion Systems, Oxford, UK) during the period of 0.08 s was rejected for the analysis.

#### Statistical analysis

Paired *t*-tests (Snedecor & Cochran, 1989) were conducted to compare mean values between C1 and C2. Significance was set at  $p \leq 0.01$ .

### 3. Results

The numbers of the trials analysed for the participants from *a* to *g* were 20, 15, 23, 14, 17, 14, and 24, respectively. All the participants threw a ball in a three-quarters delivery. The mean ball speed for each participant ranged from 32.6 m/s to 25.5 m/s, and the mean value of the mean ball speeds for all participants was  $28.9 \pm 2.9$  m/s. **Figure 4** presents the mean values of the muscle flexion torques at the wrist joint with the ranges of one SD determined under C1 and C2 for all participants. The mean value of the torque under C1 was significantly different from and larger than the value under C2 at the same sampling time from  $-0.040$  s to  $-0.002$  s ( $p < 0.001$ ) for all participants. The maximum difference between the mean values of the torque determined under C1 and C2 at the same sampling time for each participant ranged from 10.6 Nm to 15.5 Nm. The mean value of the maximum differences was  $13.7 \pm 1.9$  Nm.

Results concerning the ball kinetics or the projected first three terms on the right side of Equations (1) and (2) along the flexion-extension axis of the wrist joint will be shown hereafter to reveal reasons for the difference between the muscle flexion torques at the wrist joint determined under C1 and C2: the difference between the flexion torques determined under C1 and C2 was due to the difference between the ball kinetics determined under both conditions because the hand kinetics under C1 was the same with that under C2. **Figure 5** presents the mean values of the sum of the three elements (SUM) with the ranges of one SD determined under C1 and C2 for all participants. The mean value of the sum of the elements under C1 was significantly different from and larger than the value un-

der C2 at the same sampling time from  $-0.040$  s to  $-0.002$  s ( $p < 0.001$ ) for all participants.

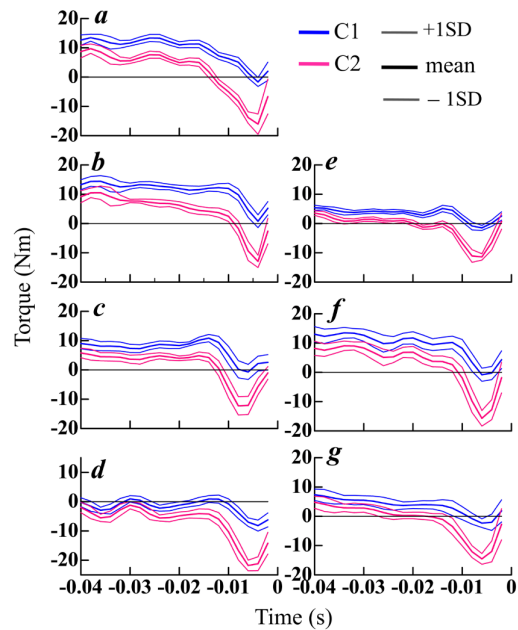


**Figure 4.** The mean values of the muscle flexion torque at the wrist joint with the ranges of one SD determined under C1 and C2 for all participants. Time 0 indicates ball release. The alphabetical letter at the upper-left side of each panel indicates a participant among the seven participants (*a - g*).

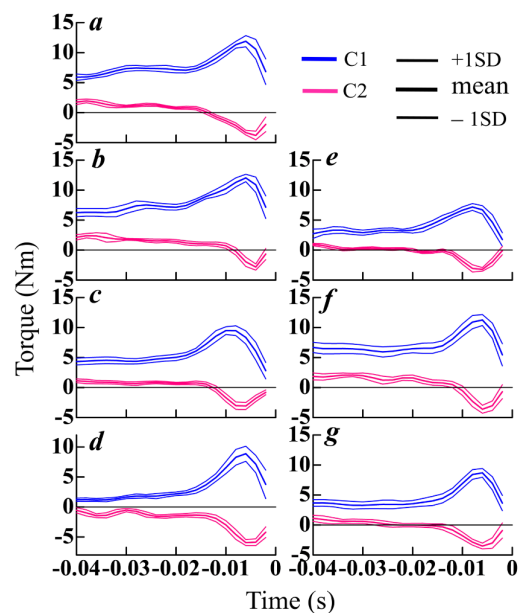


**Figure 5.** The mean torque values of the sum of the elements due to ball acceleration, due to ball angular acceleration, and due to gravity on the ball of the muscle flexion torque at the wrist joint with the ranges of one SD determined under C1 and C2 for all participants. Time 0 indicates ball release. The alphabetical letter at the upper-left side of each panel indicates a participant among the seven participants (*a - g*).

**Figure 6** presents the mean values of the sum (SUM) and its three elements with the ranges of one SD under C1 and C2 for the participant *a*. The mean value of the element due to ball acceleration (E1) under C1 was significantly different from the value under C2 ( $p < 0.001$ ) at the same sampling time (**Figure 6(b)**). The curves of the elements under C1 and C2 (**Figure 6(b)**) demonstrate patterns of the curves similar to those of their matching of the sum (**Figure 6(a)**). The mean value of the element due to ball angular acceleration (E2) under C1 started to decrease before  $-0.020$  s and indicated negative values after  $-0.018$  s until  $-0.002$  s (**Figure 6(c)**). The absolute mean values of the element due to gravity on the ball (E3) under C1 and C2 (**Figure 6(d)**) were not significant compared to the mean values of the sum under C1. The difference between the values of the sums under C1 and C2 was attributable mainly to the difference between the values of the element due to ball acceleration under C1 and C2.

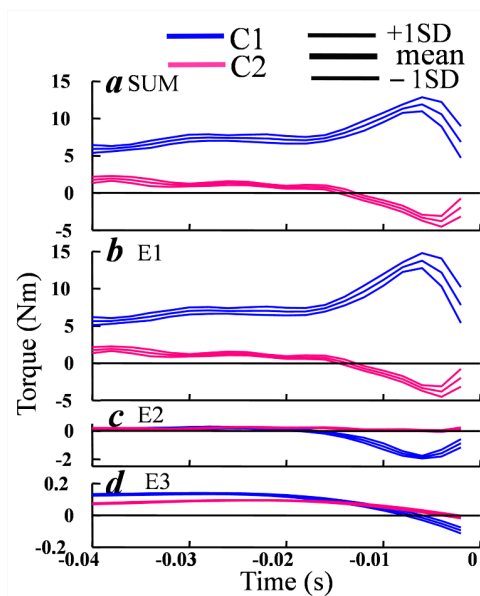


**Figure 6.** The mean torque values of the sum of the following three elements (SUM), element due to ball acceleration (E1), element due to ball angular acceleration (E2), and element due to gravity on the ball (E3) from the top panel to the bottom, with the ranges of one SD determined under C1 and C2 for the participant *a*. Time 0 indicates ball release. Note that not all the scales of the columns are the same.

**Figure 7** demonstrates the mean values of the sums of the three elements (SUM) and the three elements under C1 and C2 for all participants. The patterns of the mean curves of the three elements for the participants *b* to *g* were similar to the patterns of their matching elements for the participant *a* (**Figure 6**).

**Figure 8** demonstrates the differences between the mean values of the sum of the element due to ball acceleration (E1), element due to ball angular acceleration (E2), and element due to gravity on the ball (E3) determined under C1 and C2, and the differences between the mean values of the sum of the element due to ball angular acceleration (E2) and element due to gravity on the ball (E3) determined

under C1 and C2 at the same sampling time for all participants. The absolute values of the latter sum were small until around  $-0.020$  s, and the sum became negative after the time. The differences between the values of the sum of the three elements under C1 and C2 were attributable mainly to the differences between the values of the element due to ball acceleration under C1 and C2 because the differences between the values of the sum of the element due to ball angular acceleration and element due to gravity on the ball under C1 and C2 were considerably smaller than the differences between the values of the sum of the three elements under C1 and C2 for all participants.

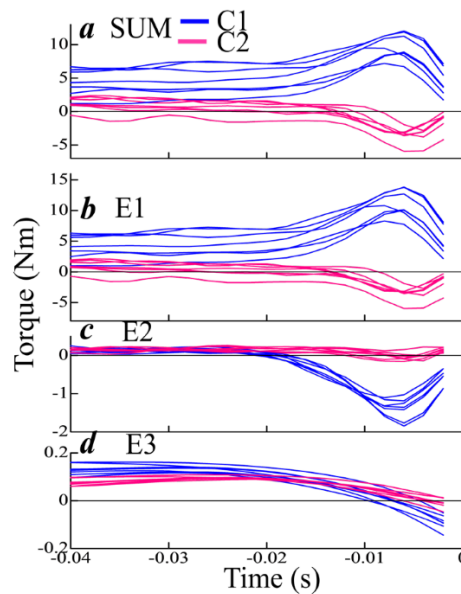


**Figure 7.** The mean torque values of the sum of the following three element (SUM), element due to ball acceleration (E1), element due to ball angular acceleration (E2), and element due to gravity on the ball (E3) from the top panel to the bottom, determined under C1 and C2 for all participants. Time 0 indicates ball release. Note that not all the scales of the columns are the same.

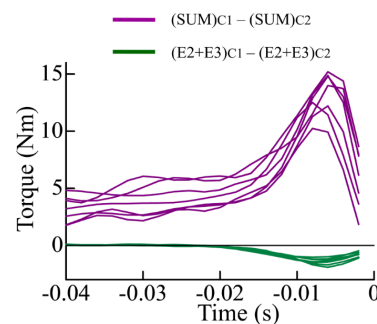


**Figure 8.** The differences between the mean values of the sum of the element due to ball acceleration (E1), element due to ball angular acceleration (E2), and element due to gravity on the ball (E3) determined under C1 and C2, and the differences between the mean values of the sum of the element due to ball angular acceleration (E2) and element due to gravity on the ball (E3) determined under C1 and C2 for all participants. Time 0 indicates ball release.

Sets of the vectors of  $r'_{fa}$ ,  $r'_b$ ,  $r'_h$ ,  $m_b a'_b$  and  $m_b a'_h$  (Kinetics section in the Methods, and Supplementary Material S3) at several sampling times in a throw by the participant *a* are presented in **Figure 9**. These sets would elucidate why the magnitude of the element due to ball acceleration (E1) under C1 is larger than that of the element under C2 at the same sampling time. The mean magnitudes of  $r'_b$  and  $r'_h$ , the differences between the mean magnitudes of the two vectors, and one SD of the differences between the magnitudes of  $r'_b$  and  $r'_h$  at the same sampling times for each participant are presented in **Figure 10(a)**, **Figure 10(b)**, and **Figure 10(c)**, respectively. The mean magnitude of  $r'_b$  was significantly different from ( $p < 0.001$ ) (**Figure 10(b)**, **Figure 10(c)**) and larger than (**Figure 10(a)**) that of  $r'_h$  at the same sampling time for each participant. The mean magnitudes of  $m_b a'_b$  and  $m_b a'_h$ , the differences between the mean magnitudes of the two vectors, and one SD of the differences between the magnitudes of  $m_b a'_b$  and  $m_b a'_h$  at the same sampling times for each participant are presented in **Figure 11(a)**, **Figure 11(b)**, and **Figure 11(c)**, respectively. The values of the differences between the magnitudes turned from positive to negative at approximately  $-0.012$  s (**Figure 11(b)**). The magnitude of  $m_b a'_b$  was significantly different from ( $p < 0.001$ ) (**Figure 11(b)**, **Figure 11(c)**) and larger than (**Figure 11(a)**) that of  $m_b a'_h$  until approximately  $-0.014$  s at the same sampling time, and the former became significantly different from ( $p < 0.001$ ) and smaller than the latter after approximately  $-0.010$  s at the same sampling time for each participant. The values of the sines of the angles between  $r'_b$  and  $m_b a'_b$  ( $\theta_1$ ) and  $r'_h$  and  $m_b a'_h$  ( $\theta_2$ ) were determined for all participants. The mean values of  $\sin\theta_1$  and  $\sin\theta_2$ , the differences between the two mean values, and one SD of the differences between the values of  $\sin\theta_1$  and  $\sin\theta_2$  at the same sampling times for each participant are presented in **Figure 12(a)**, **Figure 12(b)**, and **Figure 12(c)**, respectively. The mean value of  $\sin\theta_1$  was significantly different from (**Figure 12(b)**, **Figure 12(c)**) and larger than (**Figure 12(a)**) that of  $\sin\theta_2$  at the same sampling time from  $-0.040$  s to  $-0.002$  s for all participants ( $p < 0.001$ , except for a sampling time for the participants *b* and *e*,  $0.001 < p < 0.01$ ).

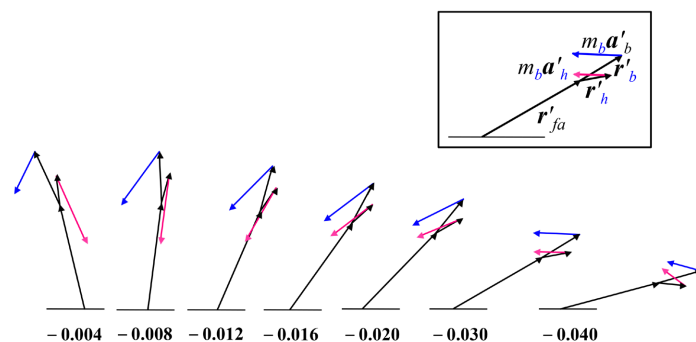


**Figure 9.** Sets of the vectors of  $r'_{fa}$ ,  $r'_b$ ,  $r'_h$ ,  $m_b a'_b$  and  $m_b a'_h$  at several sampling times in a throw by the participant *a*. The horizontal line shown under each set is parallel to the plane defined with x- and y-axes of the global coordinate system. The numerical value shown under each set indicates the time from ball release in second.

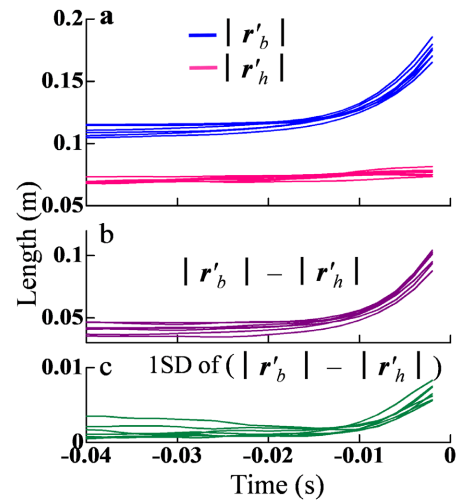


**Figure 10.** The mean magnitudes of  $r'_b$  and  $r'_h$  determined under C1 and C2, respectively (a), the differences between the mean magnitudes of the vectors (b), and one SD of the differences (c) at the same sampling times for each participant. Time 0 indicates ball release. Note that not all the scales of the columns are the same.

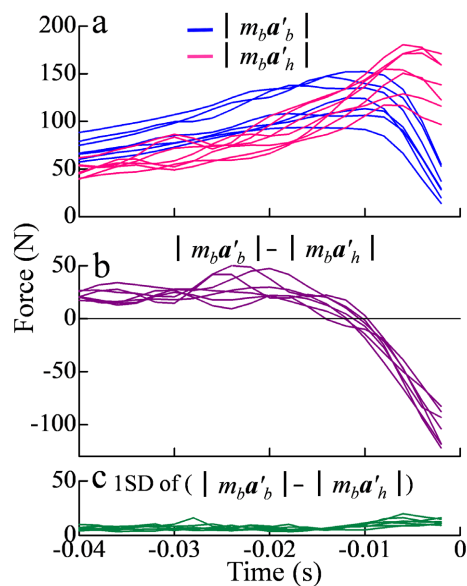


**Figure 11.** The mean magnitudes of  $m_b a'_b$  and  $m_b a'_h$  determined under C1 and C2, respectively (a), the differences between the mean magnitudes of the vectors (b), and one SD of the differences (c) at the same sampling times for each participant. Time 0 indicates ball release.

**Figure 13** demonstrates the components of the projected vectors of  $T_1$  and  $T_2$  in Equations (1) and (2), respectively, along the radial-ulnar deviation axis of the wrist joint with the ranges of one SD for all participants. **Figure 14** demonstrates the sums of the three elements determined through the projection of both first three terms on the right side of Equations (1) and (2) along the axis with the ranges of one SD for all participants. The inter-individual variation in the relationship of

the sums under C1 and C2 was considerably larger than that in the relationship of the sums determined through the projection of both first three terms along the flexion-extension axis (Figure 5).

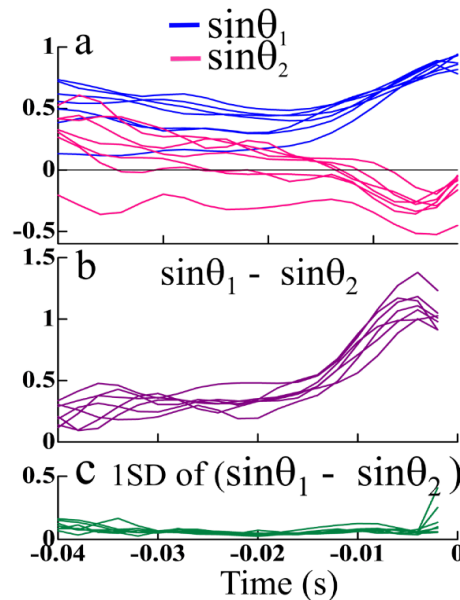


**Figure 12.** The mean values of  $\sin\theta_1$  and  $\sin\theta_2$  determined under C1 and C2, respectively (a), the differences between the mean values (b), and one SD of the differences (c) at the same sampling times for each participant. Time 0 indicates ball release.

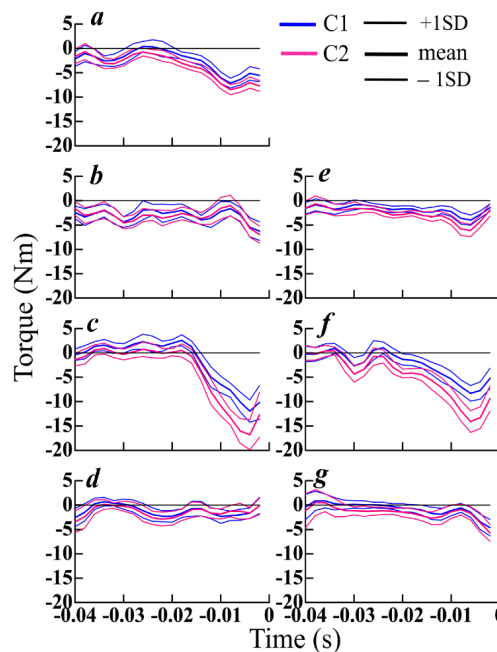


**Figure 13.** The mean values of the muscle radial (+)-ulnar (-) deviation torque at the wrist joint with the ranges of one SD determined under C1 and C2 for all participants. Time 0 indicates ball release. The alphabetical letter at the upper-left side of each panel indicates a participant among the seven participants (a - g).

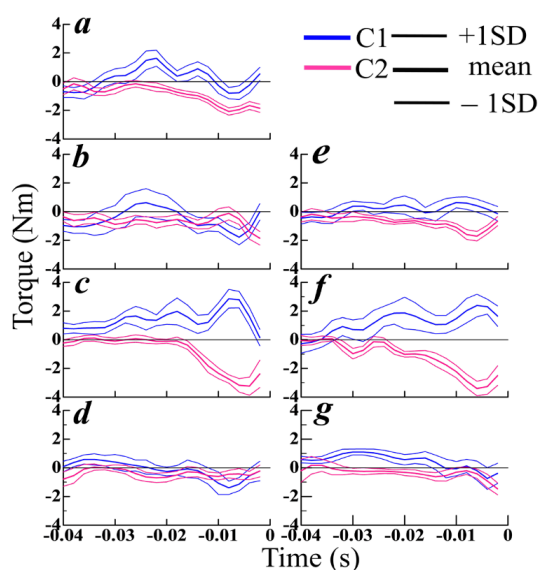


**Figure 14.** The mean torque values of the sum of the elements due to ball acceleration, due to ball angular acceleration, and due to gravity on the ball of the muscle radial (+)–ulnar (–) deviation torque at the wrist joint with the ranges of one SD determined under C1 and C2 for all participants. Time 0 indicates ball release. The alphabetical letter at the upper-left side of each panel indicates a participant among the seven participants (*a* - *g*).

#### 4. Discussion

The frame of ball release was determined as the frame next to that in which the distance between the centre of the ball and tip of the second finger was the shortest around the release in each throw. This definition is similar to that used by Matsuo et al. (2018) who have used the tip of the third finger for the determination. The tip of the second finger was adopted because the occurrence of the shortest distance for the second finger was later than or simultaneous with the occurrence for the third finger in each throw for all participants.

The inter-individual variation in the relationship of the sums of the three elements determined through the projection of both first three terms on the right side of Equations (1) and (2) along the radial-ulnar deviation axis (Figure 14) was considerably larger than that in the relationship of the sums determined through the projection of both the terms along the flexion-extension axis (Figure 5). Thus, detailed results concerning the projected components along the former axis were not reported in this paper.

The values of the muscle flexion torque at the wrist joint determined under C1 were significantly different from and larger than the values under C2 at the same sampling times from  $-0.040$  s to  $-0.002$  s for each participant (Figure 4). This result supports the hypothesis that the value of the flexion torque determined under C1 is different from that of the torque under C2 at the same sampling time for a short period immediately before ball release.

The model of the hand of the throwing arm used in this paper was assumed to be a flat rigid body in which the palm and fingers were. The muscle torque around

the wrist joint determined in this paper contained errors owing to the assumption because that the palm and fingers were not flat and that the joint angles of some fingers would change rapidly during the throwing (**Figure 4** in Kanosue et al., 2013). However, the errors did not affect the differences between the torques determined under C1 and C2 because the hand kinetics determined under C1 was the same with that under C2 as shown with both last three terms on the right side of Equations (1) and (2). Since the muscle flexion torques around the wrist joint under C1 and C2 were determined through the projection of the muscle torques around the joint  $T_1$  and  $T_2$  of Equations (1) and (2), respectively, along the flexion-extension axis of the joint, the difference between the muscle flexion torques determined under C1 and C2 was derived owing to the differences between the first three terms on the right side of Equations (1) and the terms of Equation (2). Thus, the projected components of both first three terms will be discussed hereafter to reveal reasons for the differences between the muscle flexion torques determined under C1 and C2.

The sums of the elements determined under C1 were significantly different from and larger than the sums under C2 at the same sampling times from  $-0.040$  s to  $-0.002$  s for each participant (**Figure 5**). The differences between the values of the sums under C1 and C2 at the same sampling times were considerably larger than those between the sums of the values of the elements due to ball angular acceleration and due to the gravity on the ball under C1 and C2 at the same sampling times (**Figure 8**). This indicates that the differences between the values of the sums of the elements under C1 and C2 were derived mainly from the differences between the values of the elements due to ball acceleration under C1 and C2. Thus, results concerning reasons for the latter differences will be discussed to identify reasons for the former differences. Because the values of the elements due to ball acceleration under C1 and C2 are equal to the values of  $|r'_b| \cdot |m_b a'_b| \cdot \sin \theta_1$  and  $|r'_h| \cdot |m_b a'_h| \cdot \sin \theta_2$ , respectively, as stated in the kinetics part of the Methods (Supplementary Material S3), the comparisons of the values of  $|r'_b|$  and  $|r'_h|$ ,  $|m_b a'_b|$  and  $|m_b a'_h|$ , and  $\sin \theta_1$  and  $\sin \theta_2$  may suggest reasons for the differences between the values of the elements due to ball acceleration under C1 and C2.

The mean magnitude of  $r'_b$  was larger than that of  $r'_h$  at the same sampling time from  $-0.040$  s to  $-0.002$  s for each participant (**Figure 10(a)**), and the difference between the magnitudes of  $r'_b$  and  $r'_h$  increased after approximately  $-0.020$  s (**Figure 10(b)**). This simply indicates that the distance between the COM of the ball and wrist joint centre is longer than that between the COM of the hand and centre before approximately  $-0.020$  s, and that the former distance started to increase because the ball is rolling toward the finger tips after the time. A larger magnitude of  $r'_b$  is one of the reasons that the magnitude of  $r'_b \times m_b a'_b$  is larger than that of  $r'_h \times m_b a'_h$ .

The mean magnitude of  $m_b a'_b$  was larger than that of  $m_b a'_h$  until approximately  $-0.010$  s at the same sampling time for each participant (**Figure 11(a)**) or the difference between the mean magnitudes of  $m_b a'_b$  and  $m_b a'_h$  was positive until then (**Figure 11(b)**). This was because the magnitude of  $r'_b$  was larger than

that of  $r'_h$  until approximately  $-0.010$  s, and the relative acceleration of the COM of the ball to the wrist joint centre is depicted as  $\alpha'_h \times r'_b$  and  $\alpha'_h \times r'_h$  for C1 and C2, respectively, where  $\alpha'_h$  is the angular acceleration of the hand around the wrist flexion-extension axis. A smaller magnitude of  $m_b a'_h$  is one of the reasons that the magnitude of  $r'_h \times m_b a'_h$  is smaller than that of  $r'_b \times m_b a'_b$  until  $-0.010$  s.

The mean magnitude of  $m_b a'_h$  was larger than that of  $m_b a'_b$  at the same sampling time at and after  $-0.008$  s for each participant (**Figure 11(a)**) or the difference between the mean magnitudes of  $m_b a'_b$  and  $m_b a'_h$  were negative at and after the time (**Figure 11(b)**). This may indicate that the force acting on the ball from the hand and/or fingers became insufficient to keep the ball at a stable point in the hand (Hore & Watts, 2011) under C1. The extended finger joints because of ball rolling might decrease the force further towards ball release, while the force acting on the ball under C2 was able to keep the ball at the COM of the hand because of the assumption of C2 (**Figure 9**). However, a larger magnitude of  $ma'_h$  did not make the magnitude of  $r'_h \times ma'_h$  large then (**Figure 7(b)**) because of the relative direction of  $ma'_h$  to the direction of  $r'_h$  (**Figure 9**,  $-0.008$  s to  $-0.002$  s) or the negative values of  $\sin\theta_2$  then (**Figure 12(a)**) (Supplementary Material, **Figure S2(d)**).

Analysing **Figure 9** and comparing the values of the sine of the angle between  $r'_h$  and  $ma'_h$  with the values between  $r'_b$  and  $ma'_b$  at the same sampling time, would reveal that the erroneous ball position relative to the wrist joint centre under C2 made the value of  $\sin\theta_2$  smaller than that of  $\sin\theta_1$  because of the direction of  $r'_h$  even when  $m_b a'_h$  was almost parallel to  $m_b a'_b$  ( $-0.030$  s to  $-0.016$  s) on the plane made by x- and z-axes of the wrist joint coordinate system (**Figure 2**). The difference between the values of  $\sin\theta_1$  and  $\sin\theta_2$  at the same sampling time started to increase before  $-0.015$  s for all the participants (**Figure 12(b)**). This indicates that the error of  $m_b a'_h$  in reflecting the direction of  $m_b a'_b$  enlarged after the time.

Some researchers have used the assumption that the COM of the ball was fixed at the centre of the third MP joint of the hand until ball release for the motion analysis of baseball throwing (Fleisig et al., 2006; Dun et al., 2008; Naito & Maruyama, 2008; Naito et al., 2014). The muscle flexion torque at the wrist joint determined on the assumption might contain similar amounts of errors to those determined in the present paper because the centre is close to the COM of the hand (Ae et al., 1992): the location of the COM was 89.1 % of the distance from the centre of the wrist joint to that of the third MP joint. The values of the sum of the elements determined under C2 were negative after approximately  $-0.010$  s for all participants (**Figure 7(a)**). This is similar to the results of the wrist muscle flexion torque determined using the conventional inverse dynamics analysis (Robertson et al., 2014) in baseball throwing (Miyanishi et al., 1997; Nissen et al., 2007; Hirashima et al., 2007; Jinji et al., 2012). The development of a muscle extension torque at the wrist joint immediately before ball release might partly reflect the ball kinetics in their researches.

Hirashima et al. (2008) have determined the muscle flexion torque around the wrist joint of the throwing arm in baseball pitching under C2 to determine the contribution of the torque to the angular acceleration of wrist flexion. The torque value was minus or a muscle extension torque was developed during the period from approximately  $-0.020$  s to ball release (their **Figure 9(c)**, representative single trial). This result is different from that in this paper where six participants among seven almost developed flexion torques during the period under C1 (**Figure 4**). Thus, the authors may underestimate the contribution of the flexion torque to the angular acceleration at least during the period. The maximum extension torque during the period and the period when the extension torque was developed were smaller and longer, respectively, in their paper than those determined under C2 in this paper (**Figure 4**). This may be attributable to the difference between the cutoff frequencies used for smoothing the coordinates of the body markers in 3D in their paper and this i.e., 20.1 Hz vs. 100.0 Hz; both papers have used the same type of smoothing algorithm.

Debicki et al. (2011) have determined the muscle flexion-extension torque at the wrist joint in a constrained baseball throwing where the participant sat a chair and the throwing arm almost moved in a vertical plane while the trunk was held almost stable under C2. The muscle torque reversed from flexion to extension immediately before ball release in the throw made not at slow and medium speeds, but at a fast speed. The authors also observed the EMGs simultaneously from the flexors carpi radialis and carpi ulnaris, and extensors carpi radialis and carpi ulnaris. They have considered the viscoelastic properties of the wrist as a major cause of the reversal among several possible causes. The reason for the extension torque may be that they determined the muscle flexion-extension torque at the wrist joint under C2.

Shibata et al. (2022) determined the muscle torques at the finger and wrist joints using the location of the COP at each sampling time during fastball and curveball pitches. The authors estimated the location based on the ratios among the force values at three finger points measured using a wooden ball with a built-in force sensor in aimed throwing (Shibata et al., 2018), whereas the average ball speed in the throwing was quite slower than the ball speeds of the two kinds of pitches. The finger and wrist joint torques in the former paper could have been determined without the estimation if Hof's equation had been used.

Feltner & Dapena (1986) have determined the muscle torque around the wrist joint which was necessary for determining the torques around the elbow and shoulder joints of the throwing arm in baseball pitch with their methods, although the first torque was not published in their paper. The authors assumed that the vector of the force acting on the ball from the hand or the vector's extended line passed through the COM of the ball, and that the reaction of the force acted on the hand. Although the authors did not determine the location of the COP of the force acting on the ball, the moment of the force around the wrist joint is the same with  $\mathbf{r}_b \times m_b \mathbf{a}_b$  in the Equation (1) (Supplementary Material S6). Thus, if suc-

ceeding researchers at least except for [Kaizu et al. \(2018\)](#) and [Kaizu et al. \(2020\)](#), who used the same method with that by [Feltner & Dapena \(1986\)](#), had projected the moment along the flexion-extension axis of the wrist joint, and had determined  $r'_b \times m_b a'_b$  or the element due to ball acceleration under C1, the difference between the sum of the elements (SUM) under C1 and  $r'_b \times m_b a'_b$ , which are the blue lines in [Figure 7\(a\)](#) and the lines in [Figure 7\(b\)](#), respectively, would have been considerably smaller than the difference between the SUMs under C1 and C2 ([Figure 8](#)) during the period from  $-0.040$  s to  $-0.002$  s. Some papers have not described the relative location of the baseball to the hand in the kinetic analysis of the throwing arm ([Nissen et al., 2007](#); [Solomito et al., 2014](#); [Tanaka et al., 2020](#); [Solomito et al., 2022](#); [Gomaz et al., 2024](#)). However, the information on the location is considerably important.

Some researchers investigating the kinetics of the throwing arm in baseball throwing have used the conventional inverse dynamics analysis to determine the muscle torques at the shoulder, elbow, and wrist joints. In this analysis, the wrist joint torque is determined at first. Subsequently, the torque at the adjacent proximal joint or the elbow joint is determined using the value of the adjacent distal joint or the wrist joint torque besides other parameter values. The shoulder joint torque is also determined with a similar procedure to that used for the elbow joint. Thus, the error produced at the wrist joint under C2 is accumulated in the torques at the elbow and shoulder joints. The values of the torques at these two joints determined using the conventional method for similar participants to the present may need correction when a closer investigation is required considering that the maximum differences between the mean values of the muscle flexion torque at the wrist joint determined under C1 and C2 at the same sampling time ranged from 10.6 Nm to 15.5 Nm among the participants.

The use of Lagrange's equation ([Greenwood, 1988](#)) does also not necessitate the COP to solve the inverse dynamic problem in the present paper. However, the use of Hof's equation may be simpler than that of Lagrange's in obtaining the solutions for the problem.

The inverse dynamics analysis reported by [Hof \(1992\)](#) may also be useful for the analysis of arm motions of the other events as follows: throwing motions of softball, cricket, American football, handball, basketball, bowling, throwing events in athletics, and hitting motions of racket events. The analysis may also be useful for sports training, performance optimization, and injury prevention strategies of these motions. The following two points are potential limitations of this paper. First, the participants in this paper were collegiate baseball players whose mean experience period of baseball was 9.9 years, and they threw a four-seam fastball in a three-quarters delivery. Wider populations of participants for this kind of experiment should be needed to generalize the results in this paper: varying performance levels, throwing techniques, kinds of ball speeds and rotations, and both sexes. Second, the sampling frequency of the motion capture system used in this paper was 500 Hz, and the cut-off frequency of the Butter-worth typed low-pass filter was 100 Hz. The period from the start of ball rotation relative to the hand to

ball release was approximately 0.020 s based on the angular accelerations of the hand and ball estimated from the torques acting around the y-axes of their coordinate systems (**Figure 7(c)**), and the number of frames captured during the period was approximately 10. The adoption of higher sampling and cut-off frequencies might be preferred to obtain more accurate kinetic results.

## 5. Conclusion

The value of the muscle flexion torque component due to ball kinetics around the wrist joint determined under C2 is significantly different from and smaller than the value determined under C1 at the same sampling time for at least 0.038 s immediately before ball release in baseball throwing for all the collegiate baseball players who participated in the experiment. This was mainly due to both errors in the acceleration of the COM of the ball and the position vector from the wrist joint centre to the COM of the ball under C2, suggesting that the actual ball position and motion are essential considerations to elucidate the wrist joint mechanics in the throwing. The inverse dynamics method reported by Hof (1992) which is simple and does not necessitate the location of the COP between the ball and the palm and/or finger(s) is useful for this kind of analysis.

## Acknowledgements

The author would like to thank Mr. Yoichi Iino, Ph.D. for the discussion before the start of this research. An earlier version of this paper was presented at the 64th Conference of Japan Society of Physical Education, Health and Sport Sciences in August 2013.

## Conflicts of Interest

The author declares no conflicts of interest.

## References

- Ae, M., Tang, H., & Yokoi, T. (1992). Estimation of Inertia Properties of the Body Segments in Japanese Athletes. *Biomechanisms*, *11*, 23-33. (in Japanese)  
<https://doi.org/10.3951/biomechanisms.11.23>
- Barrentine, S. W., Matsuo, T., Escamilla, R. F., Fleisig, G. S., & Andrews, J. R. (1998). Kinematic Analysis of the Wrist and Forearm during Baseball Pitching. *Journal of Applied Biomechanics*, *14*, 24-39. <https://doi.org/10.1123/jab.14.1.24>
- Debicki, D. B., Gribble, P. L., Watts, S., & Hore, J. (2011). Wrist Muscle Activation, Interaction Torque and Mechanical Properties in Unskilled Throws of Different Speeds. *Experimental Brain Research*, *208*, 115-125. <https://doi.org/10.1007/s00221-010-2465-2>
- Dun, S., Loftice, J., Fleisig, G. S., Kingsley, D., & Andrews, J. R. (2008). A Biomechanical Comparison of Youth Baseball Pitches. *The American Journal of Sports Medicine*, *36*, 686-692. <https://doi.org/10.1177/0363546507310074>
- Feltner, M. E. (1989). Three-Dimensional Interactions in a Two-Segment Kinetic Chain. Part II: Application to the Throwing Arm in Baseball Pitching. *International Journal of Sport Biomechanics*, *5*, 420-450. <https://doi.org/10.1123/ijsb.5.4.420>
- Feltner, M. E., & Dapena, J. (1989). Three-Dimensional Interactions in a Two-Segment

- Kinetic Chain. Part I: General Model. *International Journal of Sport Biomechanics*, 5, 403-419. <https://doi.org/10.1123/ijsb.5.4.403>
- Feltner, M., & Dapena, J. (1986). Dynamics of the Shoulder and Elbow Joints of the Throwing Arm during a Baseball Pitch. *International Journal of Sport Biomechanics*, 2, 235-259. <https://doi.org/10.1123/ijsb.2.4.235>
- Fleisig, G. S., Kingsley, D. S., Loftice, J. W., Dinnen, K. P., Ranganathan, R., Dun, S. et al. (2006). Kinetic Comparison among the Fastball, Curveball, Change-Up, and Slider in Collegiate Baseball Pitchers. *The American Journal of Sports Medicine*, 34, 423-430. <https://doi.org/10.1177/0363546505280431>
- Gomaz, L., van Trigt, B., van der Meulen, F., & Veeger, D. (2024). Predicting Elbow Load Based on Individual Pelvis and Trunk (Inter)segmental Rotations in Fastball Pitching. *Sports Biomechanics*. <https://doi.org/10.1080/14763141.2024.2315230>
- Greenwood, D. T. (1988). *Principles of Dynamics* (2nd ed.). Prentice-Hall, Inc.
- Hirashima, M., Kudo, K., Watarai, K., & Ohtsuki, T. (2007). Control of 3D Limb Dynamics in Unconstrained Overarm Throws of Different Speeds Performed by Skilled Baseball Players. *Journal of Neurophysiology*, 97, 680-691. <https://doi.org/10.1152/jn.00348.2006>
- Hirashima, M., Yamane, K., Nakamura, Y., & Ohtsuki, T. (2008). Kinetic Chain of Overarm Throwing in Terms of Joint Rotations Revealed by Induced Acceleration Analysis. *Journal of Biomechanics*, 41, 2874-2883. <https://doi.org/10.1016/j.jbiomech.2008.06.014>
- Hof, A. L. (1992). An Explicit Expression for the Moment in Multibody Systems. *Journal of Biomechanics*, 25, 1209-1211. [https://doi.org/10.1016/0021-9290\(92\)90076-d](https://doi.org/10.1016/0021-9290(92)90076-d)
- Hore, J., & Watts, S. (2011). Skilled Throwers Use Physics to Time Ball Release to the Nearest Millisecond. *Journal of Neurophysiology*, 106, 2024-2033. <https://doi.org/10.1152/jn.00059.2011>
- Hyodo, T. (2001). *Introduction to Classical Mechanics*. Gakujutsu Tosho Shuppansha. (In Japanese)
- Jinji, T., Ohta, K., & Ozaki, H. (2012). Multi-Body Power Analysis of the Baseball Pitching Based on a Double Pendulum. *Procedia Engineering*, 34, 784-789. <https://doi.org/10.1016/j.proeng.2012.04.134>
- Kaizu, Y., Sato, E., & Yamaji, T. (2020). Biomechanical Analysis of the Pitching Characteristics of Adult Amateur Baseball Pitchers Throwing Standard and Lightweight Balls. *Journal of Physical Therapy Science*, 32, 816-822. <https://doi.org/10.1589/jpts.32.816>
- Kaizu, Y., Watanabe, H., & Yamaji, T. (2018). Correlation of Upper Limb Joint Load with Simultaneous Throwing Mechanics Including Acceleration Parameters in Amateur Baseball Pitchers. *Journal of Physical Therapy Science*, 30, 223-230. <https://doi.org/10.1589/jpts.30.223>
- Kanosue, K., Nagami, T., Higuchi, T., Maekawa, H., & Yanai, T. (2013). Baseball Spin and Pitchers' Performance. In *31 International Conference on Biomechanics in Sports 2013*. ISBS.
- Matsuo, T., Jinji, T., Hirayama, D., Nasu, D., Ozaki, H., & Kumagawa, D. (2018). Middle Finger and Ball Movements around Ball Release during Baseball Fastball Pitching. *Sports Biomechanics*, 17, 180-191. <https://doi.org/10.1080/14763141.2016.1261932>
- Miyaniishi, T., Fujii, N., Ae, M., Kunugi, Y., & Okada, M. (1997). A Three-Dimensional Analysis on Mechanical Energy Flows of Torso and Arm Segments in Baseball Throw. *Japanese Journal of Physical Fitness and Sports Medicine*, 46, 55-67. (in Japanese) <https://doi.org/10.7600/jspfsm1949.46.55>
- Naito, K., & Maruyama, T. (2008). Contributions of the Muscular Torques and Motion-Dependent Torques to Generate Rapid Elbow Extension during Overhand Baseball Pitching. *Sports Engineering*, 11, 47-56. <https://doi.org/10.1007/s12283-008-0002-3>

- Naito, K., Takagi, H., Yamada, N., Hashimoto, S., & Maruyama, T. (2014). Intersegmental Dynamics of 3D Upper Arm and Forearm Longitudinal Axis Rotations during Baseball Pitching. *Human Movement Science, 38*, 116-132. <https://doi.org/10.1016/j.humov.2014.08.010>
- Nissen, C. W., Westwell, M., Öunpuu, S., Patel, M., Tate, J. P., Pierz, K. et al. (2007). Adolescent Baseball Pitching Technique: A Detailed Three-Dimensional Biomechanical Analysis. *Medicine & Science in Sports & Exercise, 39*, 1347-1357. <https://doi.org/10.1249/mss.0b013e318064c88e>
- O'Connell, M. E., Lindley, K. E., Scheffey, J. O., Caravan, A., Marsh, J. A., & Brady, A. C. (2022). Weighted Baseball Training Affects Arm Speed without Increasing Elbow and Shoulder Joint Kinetics. *Journal of Applied Biomechanics, 38*, 281-285. <https://doi.org/10.1123/jab.2021-0339>
- Robertson, D. G. E., Caldwell, G. E., Hamill, J., Kamen, G., & Whittlesey, S. N. (2014). *Research Methods in Biomechanics* (2nd ed.). Human Kinetics.
- Sakurai, S., Ikegami, Y., Okamoto, A., Yabe, K., & Toyoshima, S. (1993). A Three-Dimensional Cinematographic Analysis of Upper Limb Movement during Fastball and Curveball Baseball Pitches. *Journal of Applied Biomechanics, 9*, 47-65. <https://doi.org/10.1123/jab.9.1.47>
- Sakurai, S., Ikegami, Y., Yabe, K., Okamoto, A., & Toyoshima, S. (1990). Three-Dimensional Cinematographic Analysis of the Arm Movement during a Fastball Baseball Pitch. *Taiikugaku kenkyu (Japan Journal of Physical Education, Health and Sport Sciences), 35*, 143-156. (in Japanese) <https://doi.org/10.5432/jjpehss.kj00003391745>
- Shibata, S., Inaba, Y., Yoshioka, S., & Fukashiro, S. (2018). Kinetic Analysis of Fingers during Aimed Throwing. *Motor Control, 22*, 406-424. <https://doi.org/10.1123/mc.2017-0021>
- Shibata, S., Kageyama, M., Inaba, Y., Yoshioka, S., & Fukashiro, S. (2022). Kinetic Analysis of the Wrist and Fingers during Fastball and Curveball Pitches. *European Journal of Sport Science, 22*, 136-145. <https://doi.org/10.1080/17461391.2020.1866080>
- Snedecor, G. W., & Cochran W. G. (1989). *Statistical Methods* (8th ed.). Iowa State Press.
- Solomito, M. J., Cohen, A. D., Garibay, E. J., & Nissen, C. W. (2022). Lead Foot Progression Angle in Baseball Pitchers: Implications to Ball Velocity and Upper-Extremity Joint Moments. *Journal of Applied Biomechanics, 38*, 129-135. <https://doi.org/10.1123/jab.2021-0324>
- Solomito, M. J., Garibay, E. J., Woods, J. R., Öunpuu, S., & Nissen, C. W. (2014). Evaluation of Wrist and Forearm Motion in College-Aged Baseball Pitchers. *Sports Biomechanics, 13*, 320-331. <https://doi.org/10.1080/14763141.2014.955523>
- Tanaka, H., Hayashi, T., Inui, H., Muto, T., Tsuchiyama, K., Ninomiya, H. et al. (2020). Stride-Phase Kinematic Parameters That Predict Peak Elbow Varus Torque. *Orthopaedic Journal of Sports Medicine, 8*, 1-8. <https://doi.org/10.1177/2325967120968068>
- Veldpaus, F. E., Woltring, H. J., & Dortmans, L. J. M. G. (1988). A Least-Squares Algorithm for the Equiform Transformation from Spatial Marker Co-Ordinates. *Journal of Biomechanics, 21*, 45-54. [https://doi.org/10.1016/0021-9290\(88\)90190-x](https://doi.org/10.1016/0021-9290(88)90190-x)
- Zatsiorsky, V. M. (1998). *Kinematics of Human Motion*. Human Kinetics.
- Zatsiorsky, V. M. (2002). *Kinetics of Human Motion*. Human Kinetics.

## Supplementary Material

S1. Cross product of two vectors.

Right-hand rule for cross product.

The direction of the cross product of the vectors  $\mathbf{a}$  (the index finger) and  $\mathbf{b}$  (the middle finger) is perpendicular ( $\mathbf{c} = \mathbf{a} \times \mathbf{b}$ , the thumb) to the plane which  $\mathbf{a}$  and  $\mathbf{b}$  make (Figure S1(a), Figure S1(b)): the fingers are on the right hand.  $\mathbf{c}$  is upward under the positional condition of  $\mathbf{a}$  and  $\mathbf{b}$  in Figure S1(a). The positional relationship of  $\mathbf{c}$  to  $\mathbf{a}$  and  $\mathbf{b}$  does not change despite the rotation of the hand in 3D (Figure S1(b), Figure S1(c)). The magnitude of  $\mathbf{c}$  is  $|\mathbf{a}| \cdot |\mathbf{b}| \cdot |\sin \theta|$  (Figure S1(d)), where  $\theta$  is the angle between  $\mathbf{a}$  and  $\mathbf{b}$  measured in anticlockwise direction from  $\mathbf{a}$ .

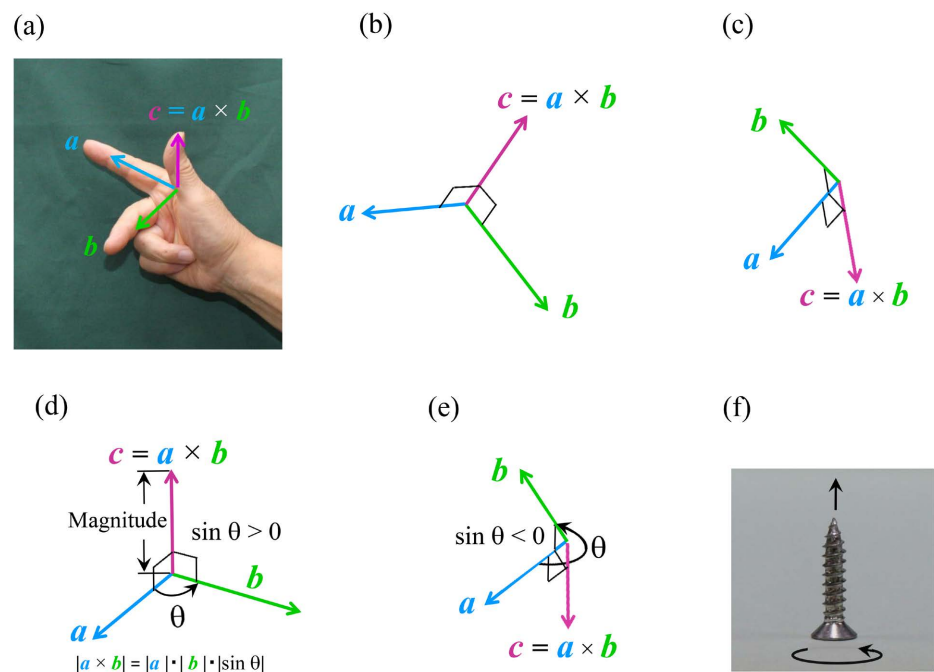


**Figure S1.** Cross product of two vectors. (a) Right-hand rule for cross product. (b) and (c) indicate that the positional relationship of  $\mathbf{c}$  to  $\mathbf{a}$  and  $\mathbf{b}$  does not change despite the rotation of the hand. (d) The definition of the magnitude of  $\mathbf{c}$ . (e) An example of  $\mathbf{c}$  when the angle between  $\mathbf{a}$  and  $\mathbf{b}$  is larger than  $\pi$  radian determined using another definition of the cross product. (f) The direction of a right-handed screw goes when turned around its long axis in anticlockwise direction from  $\mathbf{a}$  to  $\mathbf{b}$ .

Another definition of the cross product of  $\mathbf{a} \times \mathbf{b}$  is presented as follows (Hyodo, 2001):

$$\mathbf{c} = \mathbf{a} \times \mathbf{b} = |\mathbf{a}| \cdot |\mathbf{b}| \cdot \sin \theta \cdot \mathbf{e} ,$$

where  $\mathbf{e}$  is a unit vector perpendicular to  $\mathbf{a}$  and  $\mathbf{b}$ , and the direction of  $\mathbf{e}$  is the same with that of a right-handed screw goes when turned around its long axis in anticlockwise direction from  $\mathbf{a}$  to  $\mathbf{b}$  (Figure S1(f)). Thus, the direction of  $\mathbf{c}$  is perpendicularly upward to the plane made by  $\mathbf{a}$  and  $\mathbf{b}$  when  $\sin \theta > 0$  (Figure S1(d)), and perpendicularly downward to the plane when  $\sin \theta < 0$  (Figure S1(e)).

S2. Moment of a force.

When a force  $\mathbf{F}$  acts on the terminal point of a position vector  $\mathbf{r}$  (Figure S2(a)), of which initial point is at the origin (O) of a stationary orthogonal coordinate system, the cross product of  $\mathbf{r}$  and  $\mathbf{F}$  is the moment of the force around the origin. When the coordinates of  $\mathbf{r}$  and  $\mathbf{F}$  in the coordinate system are  $(x_r, y_r, z_r)$  and  $(x_F, y_F, z_F)$ , respectively (Figure S2(a)), those  $(x_{rF}, y_{rF}, z_{rF})$  of the moment of the force are as follows (Greenwood, 1988):

$$\begin{aligned} x_{rF} &= y_r \cdot z_F - z_r \cdot y_F, \\ y_{rF} &= z_r \cdot x_F - x_r \cdot z_F, \\ z_{rF} &= x_r \cdot y_F - y_r \cdot x_F. \end{aligned}$$

The position vectors  $\mathbf{r}_1$  and  $\mathbf{r}_2$ , and force vectors  $\mathbf{F}_1$  and  $\mathbf{F}_2$  in a stationary orthogonal coordinate system are projected onto the plane defined by the x- and z-axes of the orthogonal coordinate system of the wrist joint (S3), and the projected vectors are represented as  $\mathbf{r}'_1$ ,  $\mathbf{r}'_2$ ,  $\mathbf{F}'_1$ , and  $\mathbf{F}'_2$ , respectively (Figure S2(b)). Since these vectors are on the surface of the plane, the directions of  $\mathbf{r}'_1 \times \mathbf{F}'_1$  and  $\mathbf{r}'_2 \times \mathbf{F}'_2$  are perpendicular to the plane, and upward (Figure S1(b)) and downward (Figure S1(c)), respectively, according to the right hand rule of cross product, or the sign of the sine of the angle between  $\mathbf{r}'_1$  and  $\mathbf{F}'_1$  or  $\mathbf{r}'_2$  and  $\mathbf{F}'_2$  measured in anticlockwise direction (S1). This indicates  $\mathbf{r}'_1 \times \mathbf{F}'_1$  and  $\mathbf{r}'_2 \times \mathbf{F}'_2$  only have a wrist flexion component (Figure S2(c)) and a wrist extension component (Figure S2(d)), respectively, because the flexion-extension axis or y-axis is perpendicular to the plane.

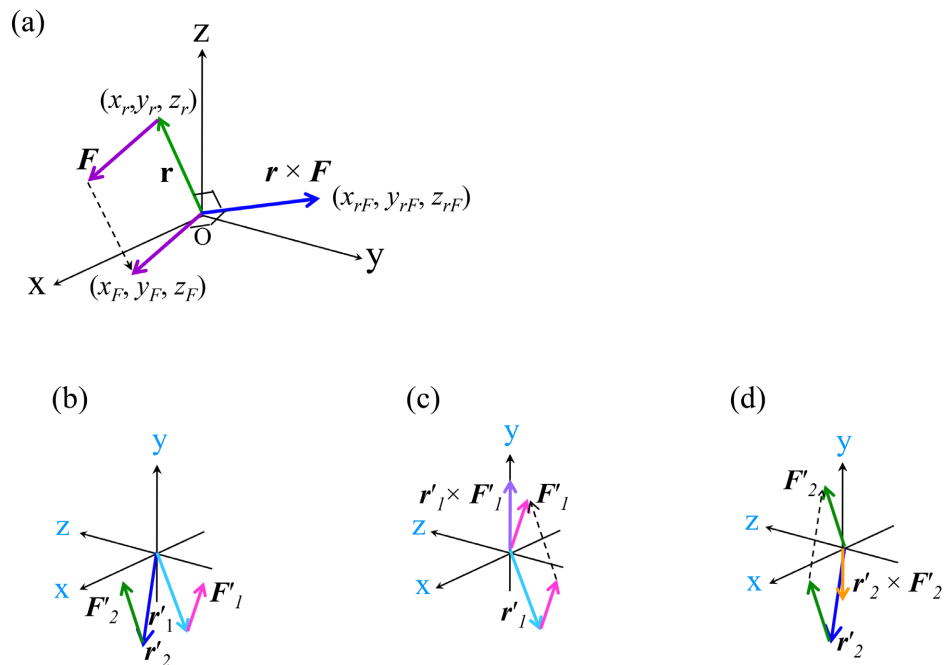
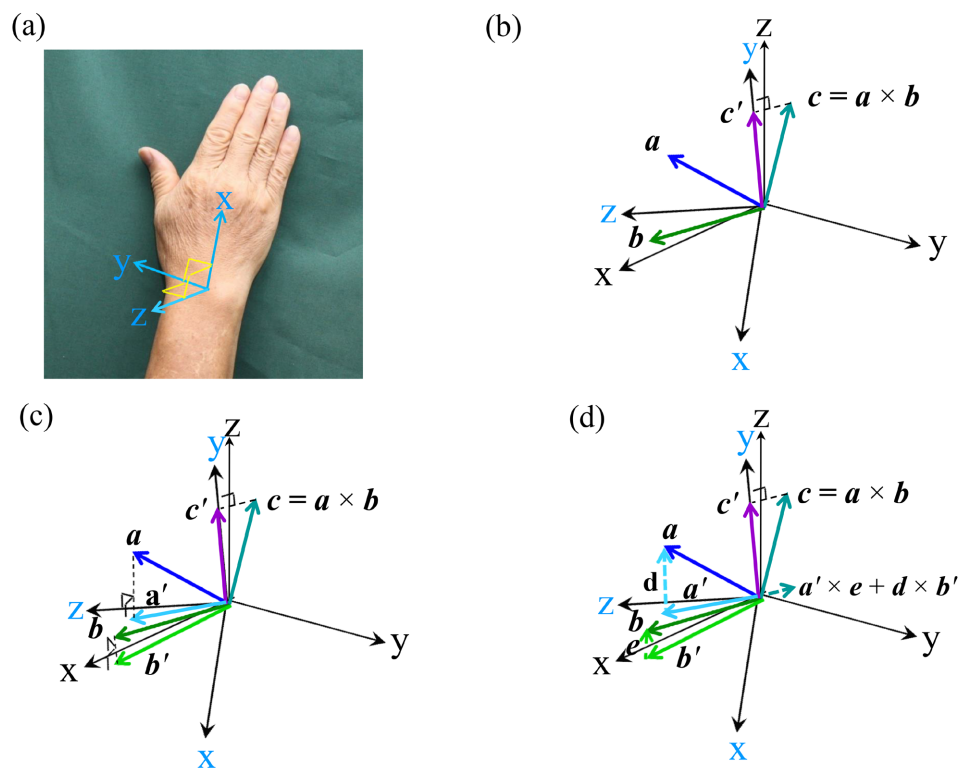


Figure S2. Moment of a force. (a) Moment of a force is determined as a cross product of a position vector  $\mathbf{r}$  and a force vector  $\mathbf{F}$  of which initial point is at the terminal point of  $\mathbf{r}$ . (b), (c), and (d). The coordinate systems are the wrist joint systems. The cross products of  $\mathbf{r}'_1$  and  $\mathbf{F}'_1$ , and  $\mathbf{r}'_2$  and  $\mathbf{F}'_2$  (b) are plus (c) and minus (d), respectively, along the y-axis.

S3. Projection of a vector in the global orthogonal coordinate system along the y-axis of the orthogonal coordinate system of the wrist joint, and onto a plane which x- and z-axes of the latter coordinate system make.

**Figure S3(a)** presents the orthogonal coordinate system of the wrist joint of the right hand, and x-, y-, and z-axes (**Table 2** in the body text). The y-axis is the flexion (+) – extension (–) axis, and the z-axis is the radial (+) – ulnar (–) deviation axis. When the vector  $\mathbf{c}$ , which is the cross product of vectors  $\mathbf{a}$  and  $\mathbf{b}$ , is projected along the y-axis, the terminal point of the projected vector  $\mathbf{c}'$  is the intersection point of the axis and the line which is perpendicular to the axis and passes the terminal point of  $\mathbf{c}$  (**Figure S3(b)**). When  $\mathbf{a}$  is projected onto a plane which the x- and z-axes make, the terminal point of the projected vector  $\mathbf{a}'$  is the intersection point of the plane and line which is perpendicular to the plane and passes the terminal point of  $\mathbf{a}$  (**Figure S3(c)**). The circumstances of the projection of  $\mathbf{b}$  onto the plane are similar to those of  $\mathbf{a}$ , and the projected vector is  $\mathbf{b}'$ .



**Figure S3.** Projection of a vector in an orthogonal coordinate system along an axis and onto a plane made with two axes of another orthogonal coordinate system. (a) The orthogonal coordinate system of the wrist joint. The y-axis is the flexion (+) – extension (–) axis, and the z-axis is the radial (+) – ulnar (–) deviation axis. (b)  $\mathbf{c}'$  is the projection of  $\mathbf{c}$  along the y-axis of the wrist joint coordinate system. (c)  $\mathbf{a}'$  and  $\mathbf{b}'$  are the projections of  $\mathbf{a}$  and  $\mathbf{b}$ , respectively, onto the plane made with x- and z-axes of the wrist joint coordinate system. (d)  $\mathbf{a}' \times \mathbf{b}' = \mathbf{c}'$ .

The cross product  $\mathbf{a}' \times \mathbf{b}'$  equals to  $\mathbf{c}'$ .  $\mathbf{a}'$  corresponds to  $r'_b$  and  $r'_h$ , and  $\mathbf{b}'$  corresponds to  $m_b a'_b$ , and  $m_b a'_h$  in **Figure 9** of the body text. Next, the reason why  $\mathbf{a}' \times \mathbf{b}'$  is equal to  $\mathbf{c}'$  will be explained. Since the vectors  $\mathbf{a}$  and  $\mathbf{b}$  are the sums

of the vectors of  $\mathbf{a}'$  and  $\mathbf{d}$ , and  $\mathbf{b}'$  and  $\mathbf{e}$ , respectively, the cross product  $\mathbf{a} \times \mathbf{b}$  equals to  $(\mathbf{a}' + \mathbf{d}) \times (\mathbf{b}' + \mathbf{e})$ , or  $\mathbf{a}' \times \mathbf{b}' + \mathbf{a}' \times \mathbf{e} + \mathbf{d} \times \mathbf{b}' + \mathbf{d} \times \mathbf{e}$  (Figure S3(d)). The vectors  $\mathbf{a}'$  and  $\mathbf{b}'$  are on the surface of the plane which the axes of z and x make, and the directions of  $\mathbf{d}$  and  $\mathbf{e}$  are perpendicular to the plane (Figure S3(d)). Both the planes which the vectors  $\mathbf{a}'$  and  $\mathbf{e}$ , and  $\mathbf{d}$  and  $\mathbf{b}'$  make are perpendicular to the plane made by z- and x-axes of the wrist joint coordinate system. Thus, the vectors of  $\mathbf{a}' \times \mathbf{e}$  and  $\mathbf{d} \times \mathbf{b}'$  are on the surface of the last plane. The cross product  $\mathbf{d} \times \mathbf{e}$  is a zero vector because the directions of both vectors are perpendicular to the plane, indicating the angle between the vectors ( $\theta$ ) is zero rad or  $\pi$  rad, i.e.  $\sin\theta = 0$  (Figure S1(d)). Hence, only  $\mathbf{a}' \times \mathbf{b}'$  among the four cross products has the component along the y-axis of the wrist joint coordinate system. The vector from the terminal point of  $\mathbf{c}'$  to that of  $\mathbf{c}$  is the sum of  $\mathbf{a}' \times \mathbf{e}$  and  $\mathbf{d} \times \mathbf{b}'$  (Figure S3(d)). Thus,  $\mathbf{a}' \times \mathbf{b}'$  is equal to  $\mathbf{c}'$ , and a component of the wrist muscle flexion torque.

#### S4. Explanations of $d(I_b \boldsymbol{\omega}_b)/dt$ and $d(I_h \boldsymbol{\omega}_h)/dt$ .

##### Nomenclature

$I_b$ and $I_h$	tensors of inertia of the baseball and hand, respectively.
$I'_b$	principal moments of inertia of the baseball around its principal axes of inertia.
$I'_{hx}$ , $I'_{hy}$ , and $I'_{hz}$	principal moments of inertia of the hand around its principal axes of inertia, or the x-, y-, and z-axes, respectively, of the hand coordinate system.
$T_{bx}$ , $T_{by}$ , and $T_{bz}$	components of $d(I_b \boldsymbol{\omega}_b)/dt$ along the x-, y- and z-axes, respectively, of the global coordinate system.
$T'_{hx}$ , $T'_{hy}$ , and $T'_{hz}$	components of $d(I_h \boldsymbol{\omega}_h)/dt$ along the x-, y- and z-axes, respectively, of the hand coordinate system.
$t$	time.
$\alpha_{bx}$ , $\alpha_{by}$ , and $\alpha_{bz}$	components of the angular acceleration of the baseball along the x-, y-, and z-axes, respectively, of the global coordinate system.
$\alpha'_{hx}$ , $\alpha'_{hy}$ , and $\alpha'_{hz}$	components of the angular acceleration of the hand along the x-, y-, and z-axes, respectively, of the hand coordinate system.
$\omega'_{hx}$ , $\omega'_{hy}$ , and $\omega'_{hz}$	components of the angular velocity of the hand along the x-, y-, and z-axes, respectively, of the hand coordinate system.
$\boldsymbol{\omega}_b$ and $\boldsymbol{\omega}_h$	angular velocities of the baseball and hand, respectively, in the global coordinate system.

$\times$ : cross product of vectors.

The bold letter indicates a vector.

An angular momentum of a rigid body around the origin of a stationary coordinate system is expressed as  $\mathbf{r} \times m\mathbf{v} + I\boldsymbol{\omega}$ , where  $m$  and  $I$  are the mass and tensor of inertia of the body, respectively,  $\mathbf{r}$  is the position vector from the origin O to the COM of the body,  $\mathbf{v}$  is the velocity vector of the COM, and  $\boldsymbol{\omega}$  is the angular velocity vector of the body (Figure S4(a)). According to the Newton-Euler equations (Zatsiorsky, 2002), the time rate of change of the angular momentum of a rigid body around the origin  $d(\mathbf{r} \times m\mathbf{v} + I\boldsymbol{\omega})/dt$  is equal to the sum of all the applied moments to the body. Thus,  $d(I\boldsymbol{\omega})/dt$  is a part of the rate of change of the body.  $d(\mathbf{r} \times m\mathbf{v} + I\boldsymbol{\omega})/dt$  is equal to  $\mathbf{r} \times m\mathbf{a} + d(I\boldsymbol{\omega})/dt$ , where  $\mathbf{a}$  is the acceleration vector of the COM, because  $d(\mathbf{r} \times m\mathbf{v})/dt = \mathbf{r} \times m\mathbf{a}$  as follows:

$$\begin{aligned} d(\mathbf{r} \times m\mathbf{v})/dt &= d\mathbf{r}/dt \times m\mathbf{v} + \mathbf{r} \times d(m\mathbf{v})/dt \\ &= \mathbf{v} \times m\mathbf{v} + \mathbf{r} \times m\mathbf{a} \\ &= \mathbf{r} \times m\mathbf{a} \end{aligned}$$

The tensor of inertia of the body  $I$  has nine elements in 3D. The values of the elements generally vary with the rotation of the body in the global coordinate system, making the process of the determination of  $d(I\boldsymbol{\omega})/dt$  complex in the kinetic analysis of rotating body segments. In the present paper, the principal moments of inertia of the hand  $I'_{hx}$ ,  $I'_{hy}$ , and  $I'_{hz}$  were used to determine  $d(I_h\boldsymbol{\omega}_h)/dt$  in the coordinate system of the hand because the values of the principal moments of inertia do not vary in spite of the rotation of the hand: the principal axes of inertia of the body overlap with the orthogonal axes of the hand coordinate system. The values of the radius of gyration of the hand (Ae et al., 1992) were used to determine the values of the principal moments of inertia. The components of  $d(I_h\boldsymbol{\omega}_h)/dt$  in the hand coordinate system (Figure 2, Table 2) were determined using Euler's equations of motion (Greenwood, 1988) as follows (Figure S4(b)):

$$\begin{aligned} T'_{hx} &= I'_{hx} \cdot \alpha'_{hx} + (I'_{hz} - I'_{hy}) \cdot \omega'_{hy} \cdot \omega'_{hz}, \\ T'_{hy} &= I'_{hy} \cdot \alpha'_{hy} + (I'_{hx} - I'_{hz}) \cdot \omega'_{hz} \cdot \omega'_{hx}, \\ T'_{hz} &= I'_{hz} \cdot \alpha'_{hz} + (I'_{hy} - I'_{hx}) \cdot \omega'_{hx} \cdot \omega'_{hy}. \end{aligned}$$

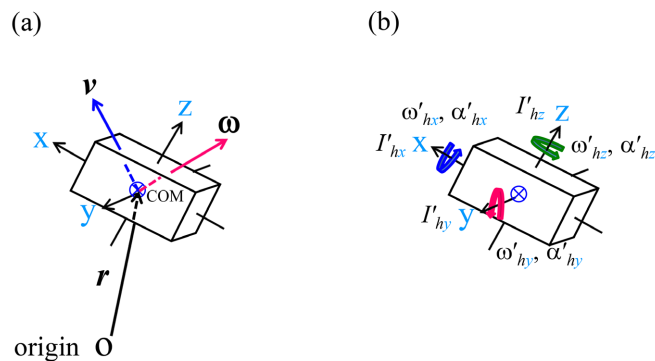


Figure S4. Explanations of  $d(I_h\boldsymbol{\omega}_h)/dt$  and  $d(I_b\boldsymbol{\omega}_b)/dt$ . (a) A panel for the understanding of the Newton-Euler equations. (b) A panel for the understanding of Euler's equations of motion.

These components were projected along the three axes of the global coordinate system first, and then projected with other parameters determined in the system along the three axes of the wrist joint coordinate system. Since the baseball is considered a homogeneous sphere, the values of the elements of  $I_b$  do not vary with the rotation of the ball in the global coordinate system when the origin of the baseball coordinate system is at the centre of the sphere (Greenwood, 1988). Thus, the components of  $d(I_b\omega_b)/dt$  for x-, y-, and z-axes in the global coordinate system are as follows:

$$T_{bx} = I'_b \cdot \alpha_{bx},$$

$$T_{by} = I'_b \cdot \alpha_{by},$$

$$T_{bz} = I'_b \cdot \alpha_{bz}.$$

In this paper, the components of  $d(I_b\omega_b)/dt$  were determined in the global coordinate system first.

### S5. Hof's equations.

#### Nomenclature

$I_b$ and $I_h$	tensors of inertia of the baseball and hand, respectively.
$m_b$ and $m_h$	masses of the baseball and hand, respectively.
$t$	time.
$\mathbf{a}_b$ and $\mathbf{a}_h$	accelerations of the centre of the masses (COMs) of the baseball and hand, respectively.
$\mathbf{F}_{b1}$ and $\mathbf{F}_{b2}$	forces acting from the palm and /or fingers on the baseball under C1 and C2, respectively, at the centre of pressure (COP) between the ball and the palm and/or fingers.
$\mathbf{F}_{h1}$ and $\mathbf{F}_{h2}$	reaction forces of $\mathbf{F}_{b1}$ and $\mathbf{F}_{b2}$ , respectively, acting from the baseball on the palm and /or fingers at the COP.
$\mathbf{F}_{w1}$ and $\mathbf{F}_{w2}$	joint forces acting from the forearm on the hand at the centre of the wrist joint under C1 and C2, respectively.
$\mathbf{g}$	acceleration due to gravity.
$\mathbf{M}_b$ and $\mathbf{M}_h$	moment acting from the palm and/or fingers on the baseball and its reaction moment acting vice versa, respectively.
$\mathbf{M}_{w1}$ and $\mathbf{M}_{w2}$	moments of the muscle forces acting from the forearm on the hand at the wrist joint under C1 and C2, respectively.
$\mathbf{r}_{bb}$ , $\mathbf{r}_{hb}$ , and $\mathbf{r}_{ww}$	positions of the COMs of the baseball and hand, and the centre of the wrist joint, respectively.
$\mathbf{r}_{cop}$	position of the COP between the baseball and palm and/or fingers.
$\mathbf{r}_p$	position of a point p which moves arbitrary.
$\mathbf{v}_b$ and $\mathbf{v}_h$	velocities of the COMs of the baseball and hand, respectively.
$\alpha_b$ and $\alpha_h$	angular accelerations of the baseball and hand, respectively.
$\omega_b$ and $\omega_h$	angular velocities of the baseball and hand, respectively.

$\times$ : cross product of vectors.

The bold letter indicates a vector.

The reason why the inverse dynamics method analysis reported by Hof (1992) does not necessitate the location of the COP of the forces acting on the palm and/or fingers from the baseball to solve the problem in this paper will be explained through the derivation of Equation (1) in the Methods section after the paper by Hof (1992). The Newton-Euler equations (Zatsiorsky, 2002) will be applied not to a rigid body recursively from the baseball to the hand but to a set of two rigid bodies composed of the hand and ball (Figure S5).

A stationary orthogonal coordinate system whose origin is O (Figure S5(a)) will be used hereafter. The initial points of the position vectors here are at the origin. According to the Newton-Euler equations, the time rate of change of the momentum of the set of the hand and baseball is equal to the sum of all the applied forces as follows (Figure S5(b)):

$$\begin{aligned} \mathbf{F}_{b1} + \mathbf{F}_{h1} + m_b \mathbf{g} + m_h \mathbf{g} + \mathbf{F}_{w1} &= d(m_b \mathbf{v}_b)/dt + d(m_h \mathbf{v}_h)/dt \\ &= m_b \mathbf{a}_b + m_h \mathbf{a}_h \end{aligned} \quad (\text{S5-1})$$

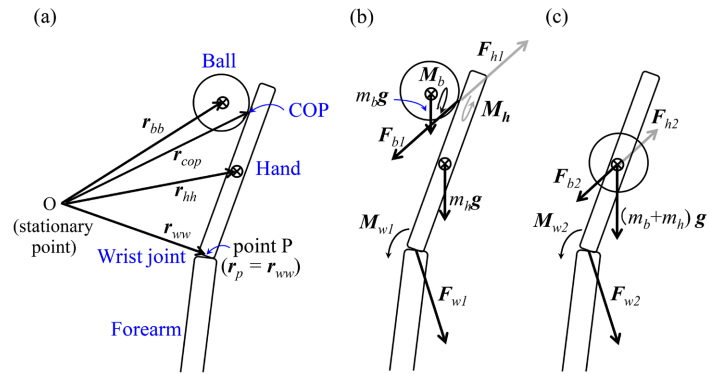


**Figure S5.** Hof's equations. (a) Position vectors from the same stationary point in the global coordinate system to the wrist joint, COMs of the hand and baseball, and COP between the hand and ball. (b) The forces and moments acting on the hand and baseball under C1. (c) The forces and moments acting on the hand and baseball under C2.

Since  $\mathbf{F}_{h1} = -\mathbf{F}_{b1}$  because  $\mathbf{F}_{h1}$  is the reaction force of  $\mathbf{F}_{b1}$ , Equation (S5-1) gives

$$\mathbf{F}_{w1} = m_b \mathbf{a}_b + m_h \mathbf{a}_h - m_b \mathbf{g} - m_h \mathbf{g} . \quad (\text{S5-2})$$

The time rate of change of the angular momentum of the set around the origin is equal to the sum of all the applied moments as follows (Figure S5(a), Figure S5(b)):

$$\begin{aligned} \mathbf{r}_{cop} \times \mathbf{F}_{b1} + \mathbf{r}_{cop} \times \mathbf{F}_{h1} + \mathbf{r}_{bb} \times m_b \mathbf{g} + \mathbf{r}_{hh} \times m_h \mathbf{g} + \mathbf{r}_{ww} \times \mathbf{F}_{w1} + \mathbf{M}_b + \mathbf{M}_h + \mathbf{M}_{w1} \\ = \mathbf{r}_{bb} \times m_b \mathbf{a}_b + \mathbf{r}_{hh} \times m_h \mathbf{a}_h + d(I_b \boldsymbol{\omega}_b)/dt + d(I_h \boldsymbol{\omega}_h)/dt \end{aligned} \quad (\text{S5-3})$$

Since  $\mathbf{M}_b = -\mathbf{M}_h$  because  $\mathbf{M}_h$  is the reaction moment of  $\mathbf{M}_b$ , and  $\mathbf{F}_{h1} = -\mathbf{F}_{b1}$ , (S5-3) gives

$$\begin{aligned} \mathbf{r}_{ww} \times \mathbf{F}_{w1} + \mathbf{M}_{w1} = \mathbf{r}_{bb} \times m_b \mathbf{a}_b + \mathbf{r}_{hh} \times m_h \mathbf{a}_h + d(I_b \boldsymbol{\omega}_b)/dt + d(I_h \boldsymbol{\omega}_h)/dt \\ - \mathbf{r}_{bb} \times m_b \mathbf{g} + \mathbf{r}_{hh} \times m_h \mathbf{g} \end{aligned} \quad (\text{S5-4})$$

By taking the cross product of  $\mathbf{r}_p$ , which is the position vector of a point p moving arbitrary, with both sides of Equation (S5-2),

$$\mathbf{r}_p \times \mathbf{F}_{w1} = \mathbf{r}_p \times m_b \mathbf{a}_b + \mathbf{r}_p \times m_h \mathbf{a}_h - \mathbf{r}_p \times m_b \mathbf{g} - \mathbf{r}_p \times m_h \mathbf{g} . \tag{S5-5}$$

The subtraction of Equation (S5-5) from Equation (S5-4) gives

$$\begin{aligned} (\mathbf{r}_{ww} - \mathbf{r}_p) \times \mathbf{F}_{w1} + \mathbf{M}_{w1} = & (\mathbf{r}_{bb} - \mathbf{r}_p) \times m_b \mathbf{a}_b + (\mathbf{r}_{hh} - \mathbf{r}_p) \times m_h \mathbf{a}_h + d(I_b \boldsymbol{\omega}_b)/dt \\ & + d(I_h \boldsymbol{\omega}_h)/dt - (\mathbf{r}_{bb} - \mathbf{r}_p) \times m_b \mathbf{g} - (\mathbf{r}_{hh} - \mathbf{r}_p) \times m_h \mathbf{g} \end{aligned} \tag{S5-6}$$

When the point p is at the centre of the wrist joint during the throwing,  $\mathbf{r}_{ww} = \mathbf{r}_p$  or  $\mathbf{r}_{ww} - \mathbf{r}_p = 0$ . Thus, Equation (S5-6) gives

$$\begin{aligned} \mathbf{M}_{w1} = & (\mathbf{r}_{bb} - \mathbf{r}_{ww}) \times m_b \mathbf{a}_b + d(I_b \boldsymbol{\omega}_b)/dt - (\mathbf{r}_{bb} - \mathbf{r}_{ww}) \times m_b \mathbf{g} \\ & + (\mathbf{r}_{hh} - \mathbf{r}_{ww}) \times m_h \mathbf{a}_h + d(I_h \boldsymbol{\omega}_h)/dt - (\mathbf{r}_{hh} - \mathbf{r}_{ww}) \times m_h \mathbf{g} \end{aligned} \tag{S5-7}$$

Since  $\mathbf{r}_{bb} - \mathbf{r}_{ww}$  and  $\mathbf{r}_{hh} - \mathbf{r}_{ww}$  are equal to  $\mathbf{r}_b$  and  $\mathbf{r}_h$  respectively (Figure 3(a)), in Equation (1) in the Methods section, Equation (S5-7) is equal to Equation (1). For the derivation of Equation (2) in the body text, the following two Equations (S5-8) and (S5-9) are used instead of Equations (S5-1) and (S5-3), respectively (Figure S5(c)):

$$\mathbf{F}_{b2} + \mathbf{F}_{h2} + (m_b + m_h) \mathbf{g} + \mathbf{F}_{w2} = d[(m_b + m_h) \mathbf{v}_h]/dt = (m_b + m_h) \mathbf{a}_h , \tag{S5-8}$$

$$\begin{aligned} \mathbf{r}_{hh} \times \mathbf{F}_{b2} + \mathbf{r}_{hh} \times \mathbf{F}_{h2} + \mathbf{r}_{hh} \times (m_b + m_h) \mathbf{g} + \mathbf{r}_{ww} \times \mathbf{F}_{w2} + \mathbf{M}_{w2} \\ = \mathbf{r}_{hh} \times (m_b + m_h) \mathbf{a}_h + d[(I_b + I_h) \boldsymbol{\omega}_h]/dt \end{aligned} \tag{S5-9}$$

The way of the derivation of Equation (2) in the body text is similar to that of Equation (1). Thus, the inverse dynamics analysis method reported by Hof (1992) does not necessitate the location of the COP of the forces acting from the baseball on the palm and/or fingers in this paper, owing to the adoption of a set of two contiguous rigid bodies and the operation using  $\mathbf{r}_p$ .

S6. The method for determining the muscle torque at the wrist joint of the throwing arm in baseball throwing by Feltner & Dapena (1986).

In this part, the moment of the force acting on the ball from the hand around the centre of the wrist joint (Feltner & Dapena, 1986) will be shown to be the same with the first term on the right side of Equation (1)  $\mathbf{r}_b \times m_b \mathbf{a}_b$  in the Methods section. The authors defined the hand as a rigid body. The figures here are in 3D until precisely before the end of this part.

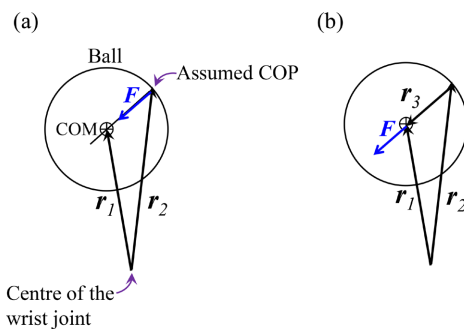


**Figure S6.** The muscle torque at the wrist joint by Feltner & Dapena (1986). (a) The force acting from the hand on the baseball. The force vector or its extended line passes the COM of the ball. (b)  $\mathbf{r}_3 \times \mathbf{F} = \mathbf{r}_1 \times \mathbf{F}$ .

According to the authors, the assumed COP in **Figure S6(a)** is the point on which the force  $\mathbf{F}$  from the hand of the throwing arm acts. The force is the product of the mass of the ball and the acceleration of the COM of the ball. The vector  $\mathbf{F}$  or its extended line passes the COM. Thus, the angular acceleration of the ball is zero. The moment of  $\mathbf{F}$  around the centre of the wrist joint is expressed as the cross product of  $\mathbf{r}_2$  and  $\mathbf{F}$  (**Figure S2(a)**) or  $\mathbf{r}_2 \times \mathbf{F}$  (**Figure S6(a)**). This moment is equal to  $\mathbf{r}_1 \times \mathbf{F}$  in **Figure S6(b)** as follows:

$$\begin{aligned}\mathbf{r}_1 \times \mathbf{F} &= (\mathbf{r}_2 + \mathbf{r}_3) \times \mathbf{F} \\ &= \mathbf{r}_2 \times \mathbf{F} + \mathbf{r}_3 \times \mathbf{F} \\ &= \mathbf{r}_2 \times \mathbf{F},\end{aligned}$$

where  $\mathbf{r}_2 + \mathbf{r}_3$  (**Figure S6(b)**) is equal to  $\mathbf{r}_1$ , and  $\mathbf{r}_3 \times \mathbf{F} = 0$  because the sine of the angle between  $\mathbf{r}_3$  and  $\mathbf{F}$  is zero (S1). Thus, the moment of the force at the assumed COP around the joint centre is equal to  $\mathbf{r}_b \times m_b \mathbf{a}_b$  in the body text. When the figures of S6(a) and S6(b) are on the plane which is perpendicular to the flexion-extension axis of the wrist joint,  $\mathbf{r}_2 \times \mathbf{F}$  is a component of the muscle flexion torque at the wrist joint (Supplementary Material S3) due to ball kinetics, and equal to  $\mathbf{r}_1 \times \mathbf{F}$  or  $\mathbf{r}'_b \times m_b \mathbf{a}'_b$  in the body text.